



**The Correlation of Periapical Radiograph, Cone Beam CT, Micro – CT and
Histologic Analysis to Evaluate Bone Quality for Dental Implant Placement**

Pradipat Suapear

**A Thesis Submitted in Partial Fulfillment of the Requirements for the Degree of
Master of Science in Oral and Maxillofacial Surgery**

Prince of Songkla University

2016

Copyright of Prince of Songkla University

Thesis Title The correlation of periapical radiograph, Cone beam CT, Micro-CT and histologic analysis to evaluate bone quality for dental implant placement.

Author Mr.Pradipat Suapear

Major Program Oral and Maxillofacial Surgery

Major Advisor :

.....
 (Assoc.Prof.Dr. Srisurang Suttapreyasri)

Co-advisor:

.....
 (Assist. Prof. Narit Leepong)

Examining Committee :

.....Chairperson
 (Asst. Prof. Dr. Suchaya Damrongsri)

.....
 (Assoc.Prof.Dr. Srisurang Suttapreyasri)

.....
 (Assist. Prof. Narit Leepong)

.....
 (Asst. Prof. Dr. Sompid Kintarak)

The Graduate School, Prince of Songkla University, has approved this thesis as partial fulfillment of the requirements for the Master of Science Degree in Oral and Maxillofacial Surgery

.....
 (Assoc.Prof.Dr.Teerapol Srichana)
 Dean of Graduate School

This is to certify that the work here submitted is the result of the candidate's own investigations.
Due acknowledgement has been made of any assistance received.

.....

(Assoc. Prof. Dr. Srisurang Suttapreyasri)

Major Advisor

.....

(Mr. Pradipat Suapear)

Candidate

I hereby certify that this work has not been accepted in substance for any degree, and is not being currently submitted in candidature for any degree.

.....

(Mr. Pradipat Suapear)

Candidate

ชื่อวิทยานิพนธ์	ความสัมพันธ์ของภาพรังสีรอบปลายราก โคนบีมคอมพิวเตดโทโมกราฟี ไมโครคอมพิวเตดโทโมกราฟีและการวิเคราะห์ทางมิถุนวิทยา เพื่อศึกษาคุณภาพกระดูกสำหรับการใส่รากฟันเทียม
ผู้เขียน	นายประดิพัทธ์ เสือเป็ย
สาขาวิชา	ศัลยศาสตร์ช่องปากและแม็กซิลโลเฟเชียล
ปีการศึกษา	2558

บทคัดย่อ

วัตถุประสงค์ เพื่อศึกษาถึงความสัมพันธ์ของข้อมูลที่ได้จากภาพรังสีรอบปลายราก โคนบีมคอมพิวเตดโทโมกราฟี ไมโครคอมพิวเตดโทโมกราฟี และการวิเคราะห์ทางมิถุนวิทยา เพื่อศึกษาคุณภาพกระดูกสำหรับการใส่รากฟันเทียม

วิธีดำเนินการวิจัย : กระดูกตัวอย่างจากตำแหน่งที่ทำการฝังรากฟันเทียมทั้งหมด 62 ตัวอย่าง แบ่งตามตำแหน่งที่ทำการศึกษา เป็นตำแหน่ง ฟันหน้าบน (12 ตัวอย่าง) ฟันหลังบน (19 ตัวอย่าง) ฟันหน้าล่าง (10 ตัวอย่าง) และ ฟันหลังล่าง (21 ตัวอย่าง) ใช้สแตนต์สำหรับถ่ายภาพรังสี เพื่อกำหนดตำแหน่งกระดูกที่ทำการศึกษา โดยนำชิ้นตัวอย่างเพื่อนำการวิเคราะห์ ความหนาของกระดูกทึบ ความหนาแน่นของกระดูก (เกรวลูจากภาพรังสีรอบปลายราก เกรเด้นซีตีวาลูจากโคนบีมคอมพิวเตดโทโมกราฟี โบนมิเนอรัล เดนซิตี โบนโวลูมแฟรคชัน, ความหนาเส้นใยกระดูก ความพรุนจากไมโครคอมพิวเตดโทโมกราฟี และความหนาแน่นของกระดูกจากการวิเคราะห์ทางมิถุนวิทยา) ทำการภาพรังสีรอบปลายราก โคนบีมคอมพิวเตดโทโมกราฟี และไมโครคอมพิวเตดโทโมกราฟี เทียบกับ การวิเคราะห์ทางมิถุนวิทยาซึ่งถือเป็นมาตรฐานสูงสุด ทำการวิเคราะห์ข้อมูลโดยใช้ การวิเคราะห์ความแปรปรวน แบบจำแนกทางเดียว สัมประสิทธิ์สหสัมพันธ์แบบเพียร์สัน การวิเคราะห์การถดถอย

ผลการวิจัย: มีความแตกต่างของ สันฐานวิทยา ระหว่างทั้ง 4 กลุ่มที่ทำการศึกษา โดยพบความหนาของกระดูกทึบมีค่า 0.87 ± 0.18 ถึง 1.19 ± 0.24 มิลลิเมตร ตำแหน่งที่มีค่าสูงสุดคือ ฟันหน้าล่าง โดยพบความแตกต่างอย่างมีนัยสำคัญระหว่างกลุ่ม ($p < 0.01$) สัมประสิทธิ์สหสัมพันธ์แบบเพียร์สันมีค่าสูงในการวัดความหนาของกระดูกทึบ ระหว่าง โคนบีมคอมพิวเตดโทโมกราฟี และไมโครคอมพิวเตดโทโมกราฟี ($r = 0.933$ $p < 0.01$) การวัดความหนาแน่นของกระดูก ภาพรังสีรอบปลายราก และ โคนบีมคอมพิวเตดโทโมกราฟี ไม่สามารถแยกความแตกต่างระหว่างกลุ่มได้ ในขณะที่ โบนมิเนอรัล เดนซิตี โบนโวลูมแฟรคชัน ความหนาเส้นใยกระดูก ความพรุนจากไมโครคอมพิวเตด

โทโมกราฟฟี และความหนาแน่นของกระดูกจากการวิเคราะห์ทางมิถุนวิทยา สามารถแยกแยะความแตกต่างระหว่างกลุ่มได้ ($p < 0.01$) โดยตำแหน่งที่มีความหนาแน่นสูงคือ กลุ่มขากรรไกรล่าง(ฟันหน้าล่าง และฟันหลังล่าง) พบมีค่าสูงกว่ากลุ่มขากรรไกรบน(ฟันหน้าบน และฟันหลังบน) ไม่พบความสัมพันธ์ระหว่างค่าเกรวาลูจากภาพรังสีรอบปลายรากกับเกรเด้นซิติ์วาลูจากโคนบีมคอมพิวเตดโทโมกราฟฟี ($r = -0.237$ $p = 0.064$) โบนมิเนอรัล เดนซิติ์ ($r = -0.039$ $p = 0.961$) โบนโวลูมแฟรคชัน ($r = 0.107$ $p = 0.408$) ความหนาแน่นไขกระดูก ($r = -0.112$ $p = 0.386$) ความพรุน ($r = -0.054$ $p = 0.676$) จากไมโครคอมพิวเตดโทโมกราฟฟี และ ความหนาแน่นของกระดูกจากการวิเคราะห์ทางมิถุนวิทยา ($r = -0.006$ $p = 0.765$). นอกจากนี้ไม่พบความสัมพันธ์ของ เกรเด้นซิติ์วาลูจากโคนบีมคอมพิวเตดโทโมกราฟฟี กับ โบนมิเนอรัล เดนซิติ์ ($r = -0.106$ $p = 0.411$) โบนโวลูมแฟรคชัน ($r = -0.057$ $p = 0.657$) ความหนาแน่นไขกระดูก ($r = -0.099$ $p = 0.444$) ความพรุน ($r = 0.033$, $p = 0.800$) จากไมโครคอมพิวเตดโทโมกราฟฟี และความหนาแน่นของกระดูกจากการวิเคราะห์ทางมิถุนวิทยา ($r = -0.135$ $p = 0.294$). พบความสัมพันธ์ในระดับสูงระหว่าง โบนมิเนอรัล เดนซิติ์ จากจากไมโครคอมพิวเตดโทโมกราฟฟีกับความหนาแน่นของกระดูกจากการวิเคราะห์ทางมิถุนวิทยา ($r = -0.812$ $p < 0.01$). จากการวิเคราะห์การถดถอย พบความสัมพันธ์ ความหนาของกระดูกที่บจากโคนบีมคอมพิวเตดโทโมกราฟฟีกับ โบนมิเนอรัล เดนซิติ์ ($r = 0.818$ $r^2 = 0.669$), โบนโวลูมแฟรคชัน ($r = 0.634$ $r^2 = 0.402$) ความหนาแน่นไขกระดูก ($r = 0.626$ $r^2 = 0.392$) ความพรุน ($r = -0.662$ $p = 0.438$) และ ความหนาแน่นของกระดูกจากการวิเคราะห์ทางมิถุนวิทยา ($r = 0.738$ $r^2 = 0.545$)

สรุปผล: ขากรรไกรล่าง(ฟันหน้าล่าง และฟันหลังล่าง) มีความหนาของกระดูกที่บและความหนาแน่นของกระดูกมากกว่าขากรรไกรบน(ฟันหน้าบน และฟันหลังบน) ตามการศึกษาจากไมโครคอมพิวเตดโทโมกราฟฟี และการวิเคราะห์ทางมิถุนวิทยา จากการศึกษาค่าเกรวาลูจากภาพรังสีรอบปลายรากและเกรเด้นซิติ์วาลูจากโคนบีมคอมพิวเตดโทโมกราฟฟี ไม่สามารถแสดงผลของความหนาแน่นของกระดูกที่แท้จริงได้เมื่อเทียบกับ ไมโครคอมพิวเตดโทโมกราฟฟี และการวิเคราะห์ทางมิถุนวิทยาซึ่งถือเป็นการตรวจมาตรฐานสูงสุด ความหนาของกระดูกที่บที่วัดจากโคนบีมคอมพิวเตดโทโมกราฟฟีพบว่ามีสัมพันธ์กับความหนาแน่นของกระดูก ซึ่งข้อมูลที่ได้ก่อนการผ่าตัดนี้ เป็นประโยชน์ต่อการแสดงถึงตัวชี้วัดในการประเมินคุณภาพของกระดูก ในตำแหน่งที่ทำการฝังรากฟันเทียม

คำสำคัญ: คุณภาพกระดูก ความหนาของกระดูกที่บ เกรวาลู เกรเด้นซิติ์วาลู โบนมิเนอรัล เดนซิติ์ โคนบีมคอมพิวเตดโทโมกราฟฟี ไมโครคอมพิวเตดโทโมกราฟฟี การวิเคราะห์ทางมิถุนวิทยา

Thesis Title: The Correlation of Periapical Radiograph, Cone Beam CT, Micro-CT and Histologic Analysis to Evaluate Bone Quality for Dental Implant Placement

Author: Mr. Pradipat Suapear

Major program: Oral and Maxillofacial Surgery

Academic Year: 2015

ABSTRACT

Objectives: To determine the correlation of the bone morphology parameters measured using periapical radiography, cone-beam computed tomography (CBCT), micro-computed tomography (micro-CT) and histologic assessment to evaluate bone quality for dental implant placement.

Materials and methods: Sixty-two bone samples were grouped according to the region of harvesting: upper anterior (UA: n=12), upper posterior (UP: n=19) lower anterior (LA: n=10) and lower posterior (LP: n=21). A surgical stent with a radiopaque marker located at the surgical site was used during radiographic assessments and bone core harvest. For radiographic assessment, the corresponding area for bone core harvest was localized and was analyzed for the cortical thickness, the bone density (gray value from periapical radiograph and CBCT; bone mineral density (BMD), bone volume density (BV/TV), % porosity from micro-CT; and bone density from histology). The periapical radiographic, CBCT and micro-CT assessments were compared with the histologic analyses. Data were analyzed using One-way, Pearson correlation coefficients, and simple linear regression. Inter-rater reliability was evaluated using intra-class correlation coefficients.

Results: There were the differences in bone morphology among 4 regions. The cortical thickness was range from 0.87 ± 0.18 to 1.19 ± 0.24 mm with the highest value at LA region. A statistically significant difference ($p<0.001$) was found among the cortical thickness of 4 regions. A high positive Pearson's correlation coefficient was observed between CBCT and micro-CT ($r=0.933$, $p<0.01$). For bone density assessments, the gray value from periapical radiograph and CBCT could not discriminate among different regions, while, BMD, BV/TV,

and % porosity from micro-CT, as well as, bone density from histologic analysis showed statistically significant difference ($p < 0.01$) among 4 regions with the higher density in mandible (LA and LP) groups than maxilla (UA and UP) groups. There was no correlation between gray value from periapical radiograph and CBCT ($r = -0.237$, $p = 0.064$), BMD ($r = -0.039$, $p = 0.961$), BV/TV ($r = 0.107$, $p = 0.408$) nor histology measurement ($r = -0.006$, $p = 0.765$). There was also no correlation between gray value from CBCT and BMD ($r = -0.106$, $p = 0.441$), BV/TV ($r = -0.057$, $p = 0.657$) nor histology measurement ($r = -0.135$, $p = 0.294$). A high Pearson's correlation coefficient in bone density was observed between BMD and histologic analysis ($r = 0.812$, $p < 0.01$). Linear regression showed that there was a correlation between CBCT's cortical thickness and BMD ($r = 0.818$, $r^2 = 0.669$), BV/TV ($r = 0.634$, $r^2 = 0.402$), porosity ($r = -0.662$, $r^2 = 0.438$) and histologic bone density ($r = 0.738$, $r^2 = 0.545$).

Conclusions: The mandible (LA and LP) revealed the higher cortical thickness and bone density than the maxilla (UA and UP) according to the micro-CT and histologic analysis. Gray value from periapical radiograph and CBCT could not reveal the true bone density that using BMD, BV/TV, and histology assessment as the references. The cortical thickness measured from CBCT was correlated with the bone density. This pre-operative parameter could be utilized as the indicator for bone quality at the implant installation site.

Keywords: Bone quality, cortical thickness, gray values, bone mineral density, cone-beam computed tomography, Micro-Computed Tomography, histology.

ACKNOWLEDGEMENTS

This thesis in obtaining my degree in Master of Science in oral and maxillofacial surgery. I could not possibly complete this thesis without strong support from several persons who support for assistance and preparation

First of all, I would like to express my gratitude to Assoc.Prof.Dr. Srisurang Suttapreyasri (Major advisor) for her continuous and unfailing support, extensive knowledge, valuable times and advices. I will remember her great heart for giving me suggestion and goodwill during my entire study. Also Assist. Prof. Narit Leepong (advisor), for valuable samples in this thesis, vast knowledge and guiding throughout the thesis work. Especially, the scientific knowledge at the clinic.

Next, I would like to thank Mr. Kemarajt Kemavongse and all staffs at the Research center, Faculty of Dentistry, Prince of Songkla University for facilitating for specimens preparation and analysis. I would like to specially thank Miss Benjawan Triranurat who help me for the studying. Miss.Sutthinun Kongin, department of Oral Radiology for radiographs. Miss Miss.Somrudee Atthachit, Center of Nanoimaging (CNI), Faculty of Science, Mahidol University for histological images.

I would like to sincerely thank to the Oral and Maxillofacial Surgery Clinic, Faculty of Dentistry, Prince of Songkla University for the attention and support of the staffs of Department of Surgery for their kind help and assistance during my time of study. Also I would say that my deepest gratitude goes to my family that has been supporting my heart and encouraging me for this thesis.

In conclusion, I appreciate all of you that had been helping me out to the end of my master. Without you, I wouldn't finish my thesis. I will never forget your generosity and kindness.

Pradipat Suapear

CONTENTS

	Page
CONTENTS	x
LIST OF TABLES	xi
LIST OF FIGURES	xii
LIST OF ABBREVIATION AND SYMBOLS	xvi
CHAPTER	
1. INTRODUCTION	1
1.1 RATIONAL OF STUDY	1
1.2 REVIEW OF LITERATURE	2
1.3 OBJECTIVE OF THE STUDY	19
2. MATERIALS AND METHODS	20
3. RESULTS	31
4. DISCUSSION	59
5. CONCLUSION	62
REFERENCES	63
APPENDIX	75
VITAE	77

LIST OF TABLE

Table	Page
1. Comparison of characterized bone with the bone quality classifications	4
2. The correlation of various techniques for bone quality assessment	13
3. Sample investigated in this study	31
4. Summary of the bone density parameters measured from a periapical radiograph, CBCT, Micro-CT and histologic analysis	40
5. The correlation coefficient between periapical radiography gray value and other bone density parameters from CBCT, Micro-CT or histologic analysis	46
6. The correlation coefficient of gray density value of CBCT and other bone density parameters from Micro-CT or histologic analysis	50
7. The correlation coefficient of bone density parameters from Micro-CT and bone density parameters from histologic analysis	54
8. Measurement accuracy of cortical thickness of 4 regions by means, mean difference (Mean Diff), Absolute value of the mean difference (Mean Abs), standard deviations, and correlations	57
9. The correlation coefficient of cortical thickness from a CBCT and bone density parameters from a micro-CT and histologic analysis	58

LIST OF FIGURES

Figure	Page
1. Cawood and Howell classified edentulous jaws according to a three-dimensional analysis of the anatomy, focusing on the changes in shape for both vertical and horizontal axes of the alveolar process	2
2. Implant success rates as related to bone quality	5
3. Periapical radiograph and radiopaque material to localize the implant installation site. (A) Periapical radiograph after dental implant placement. (B)	7
4. Orthopantomography (OPG) represents the maxillofacial area such as the maxilla and mandibular arch, the maxillary sinus and the inferior alveolar nerve	8
5. The bone density measurement from CBCT in grayscale at the implant site	10
6. Micro- CT evaluation with 3D reconstruction of a specimen for bone quality assessment	11
7. Histologic analysis for bone density measurement	12
8. The conceptual framework of the experimental design.	21
9. Study cast for surgical stent construction (9A) Surgical stent with radiopaque markers for locating bone quality measurement(9B)	22
10. Film No2. with a custom lead step wedge (10A), the length of each lead steps (10B)	23
11. The periapical radiograph with area for gray value measurement (11A). Area for bone density measurement the cortical (2x2 mm), trabecular (2x3 mm) and total (2x5 mm) gray value measurement underneath radiopaque marker from periapical radiograph (11B). Image J program for gray value measurement from periapical radiograph (11C).	24

LIST OF FIGURES (CONTINUED)

Page		Figure
12.	Radiographic stent with the parallel hole filled with radiopaque material to locate the position for bone density measurement (12A) One volume viewer program for gray density measurement from CBCT to locate the position for bone density measurement (12B)	25
13.	Bone trephine for micro-CT and histologic analysis(13A and 13B)	26
14.	Bone specimen from trephine bur (14A) Holder of specimen for micro-CT scanning. (14B) Micro-CT (Scanco 35, Scanco Medical AG, Switzerland) (14C)	27
15.	The specimens were dehydrated using ascending grades of alcohol, infiltrated and embedded in methylmethacrylate (MMA)	28
16.	The specimens were embedded in MMA and completed polymerization for undecalcified sectioning	28
17.	Cutting and grind machine for undecalcified sectioning	29
18.	The specimen was stained with toluidine blue.	29
19.	Histologic preparation and stained with Toluidine blue for the measurement percentage area of cortex and trabecular bone	30
20.	The comparison of the image received from the periapical radiograph (20a), CBCT (20b), micro-CT (20c, 20d) and histologic analysis (20e) from the upper anterior region (UA)	33
21.	The comparison of the image received from a periapical radiograph (21a), CBCT (21b), micro-CT (21c,21d) and histologic analysis (23e) from UP	35
22.	The comparison of the image received from a periapical radiograph (22a), CBCT (22b), micro-CT (22c,22d) and histologic analysis (22e) from LA	37

LIST OF FIGURES (CONTINUED)

Figure	Page
23. The comparison of the image received from a periapical radiograph (23a), CBCT (23b), micro-CT (25c,25d) and histologic analysis (25e) from LP	39
24. Total, cortical and trabecular gray value from periapical radiograph in each group	41
25. Total, cortical and trabecular gray density value from CBCT in each groups	42
26. BV/TV (%) from Micro-CT in each groups	42
27. Trabecular thickness (mm) from Micro-CT in each groups	43
28. Porosity (%) from Micro-CT in each groups	43
29. Bone mineral density (mg/ccm) from Micro-CT in each groups	44
30. Cortical bone density (%) from histologic analysis in each groups	44
31. Trabecular bone density (%) from histologic analysis in each groups	45
32. Total bone density (%) from histologic analysis in each groups	45
33. The correlation coefficient between gray value from periapical radiograph and gray density value from CBCT.	47
34. The correlation coefficient between gray value from periapical radiograph and BV/TV from Micro-CT	47
35. The correlation coefficient between gray value from periapical radiograph and trabecular thickness from Micro-CT.	48
36. The correlation coefficient between gray value from periapical radiograph and porosity from Micro-CT	48
37. The correlation coefficient between gray value from periapical radiograph and bone mineral density from Micro-CT	49

LIST OF FIGURES (CONTINUED)

Figure		Page
38.	The correlation coefficient between periapical radiography gray value and bone density from histologic analysis	49
39.	The correlation coefficient between gray density value from CBCT and BV/TV from Micro-CT	51
40.	The correlation coefficient between gray density value from CBCT and trabecular thickness from Micro-CT	51
41.	The correlation coefficient between gray density value from CBCT and porosity from Micro-CT	52
42.	The correlation coefficient between gray density value from CBCT and bone mineral density from Micro-CT	52
43.	The correlation coefficient between gray density value from CBCT and bone density from histologic analysis	53
44.	The correlation coefficient between BV/TV from Micro-CT and bone density from histologic analysis	55
45.	The correlation coefficient between bone mineral density from Micro-CT and bone density from histologic analysis	55
46.	The correlation coefficient between porosity from Micro-CT and bone density from histologic analysis	56

LIST OF ABBREVIATION AND SYMBOLS

ANOVA	=	One-way analysis of variance
kVp	=	Kilovoltage peak
mA	=	Milliampere
OPG	=	Orthopantomography
CBCT	=	Cone beam computed tomography
Micro-CT	=	Micro computed tomography
MSCT	=	Multislice computed tomography
CT	=	Computed tomography
FOV	=	Field of view
mm	=	Millimeter
HU	=	Hounsfield Unit
ROI	=	Region of interest
SD	=	Standard deviation
UA	=	Upper anterior
UP	=	Upper posterior
LA	=	Lower anterior
LP	=	Lower posterior
BIC	=	Bone implant contact
BIV	=	Bone implant volume
BV	=	Bone volume
BS	=	Bone surface
Tb.Sp	=	Trabecular separation
Tb.Th	=	Trabecular thickness
Tb.N	=	Trabecular numbers
W	=	Watt
2D	=	Two- dimension
3D	=	Three-dimension
No.	=	Number

LIST OF ABBREVIATIONS AND SYMBOLS (CONTINUED)

AAOMR	=	Academy of Oral and Maxillofacial Radiology
MMA	=	Methyl methacrylate
Diff	=	Difference
Mean Abs	=	Absolute value of the mean difference

CHAPTER 1

INTRODUCTION

Rational of study

Successfully delivering dental implants to patients who have lost teeth and the surrounding bone relies on the careful gathering of clinical and radiological information, in particular, bone quantity and bone quality. Low bone quality, being thin cortical bone and low-density trabecular bone, is one of the factors associated with implant failures from biological causes¹, for example, failure to establish osseointegration before implant loading and failure to maintain the osseointegration after implant loading². Therefore, the bone quality should be determined prior to the implant placement, in the pre-surgical planning.

Previously, periapical radiographs along with orthopantomograph (OPG) were used for diagnosing and treatment planning. However, a periapical radiograph and panoramic image provides only a 2-dimensional (2D) view of 3-dimensional (3D) structures, which can lead to underestimation of bone loss. Accurate assessment of hard tissue morphology and density are impossible because of the variable distortions occurring in different parts of a radiograph and additionally, it is unable to provide a cross-sectional dimension³. Recently, multi-slice computed tomography (MSCT), as well as cone-beam computed tomography (CBCT), are increasingly considered fundamental for optimal dental implant placement^{4,5}. However, high cost and higher radiation exposure risk to patients in comparison with other equipment remains the main concern when using MSCT for assessing bone quality⁶⁻⁹. CBCT, as compact equipment, is more accessible to dental practitioners. It has less cost and radiation dosage and has widely replaced MSCT for oral and maxillofacial imaging. CBCT offers a radiographic method for a structural and qualitative analysis of the bone¹⁰⁻¹². Several studies reported the high geometric accuracy of CBCT for linear measurement¹³⁻¹⁵, nevertheless, the validity and reliability of bone quality evaluation remain controversial¹⁶⁻²⁰.

It is therefore considered that information gathered from a bone specimen is a more precise evaluation of bone density. However, since the use of periapical radiography and CBCT are non-invasive, it can provide a pre-operative diagnosis in dental implant placement. It is clinically of great significance to analyze the correlation between the periapical radiograph, CBCT and genuine bone specimen (Micro-CT and histologic analysis).

Review of the literatures

Bone quantity

Bone quantity measurements of the jawbone are categorized into 5 groups based on residual jaw shape and different rates of bone resorption following tooth extraction²¹. During all stages of atrophy of the alveolar ridge, characteristic shapes result from the resorption process. Cawood and Howell²² classified edentulous jaws according to a 3D analysis of the anatomy, focusing on the changes in shape for both vertical and horizontal axes of the alveolar process (Figure 1).

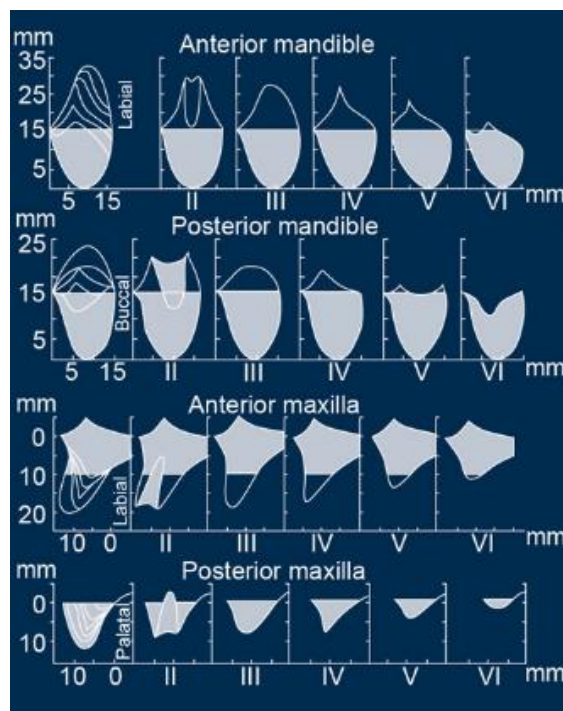


Figure 1: Cawood and Howell²² classified edentulous jaws according to a 3D analysis of the anatomy, focusing on the changes in shape for both vertical and horizontal axes of the alveolar process

Bone quality





The bone quality comprises the thickness of the cortical bone and patterns of trabecular bones. Bone quality is not only a matter of mineral content but also of a structure such as skeletal size, the architecture, the 3D orientation of the trabeculae and the matrix properties²³. It has been shown that bone density (bone mineral density, BMD) is a suitable measurable parameter for evaluating bone quality at the dental implant installation site²⁴.

Classification of bone quality

There are various classifications described for bone quality assessment. The first subjective classification was introduced by Lekholm & Zarb²⁵ in 1985. They categorized bone into 4 classes (Q1-Q4) using bone morphology. Q1: most of the entire jaw is comprised of homogenous compact bone, Q2: a thick layer of compact bone surrounds a core of dense trabecular bone, Q3: a thin layer of cortical bone surrounds a core of dense trabecular bone, Q4: a thin layer of cortical bone surrounds a core of low-density trabecular bone (Table 1).

Clinically, bone quality is evaluated by bone density using tactile perception during the preparation of the implant site^{26,27}. This subjective approach permits the adaptation of the surgical sequence before the insertion of the implant, and classification has also been used to characterize bone density by perception during drilling procedures for detecting bone quality^{26,28}. Rebaudi and coworker²⁹ classified bone density into 3 subjective bone quality: hard, normal and soft bone. Misch³⁰ defined 4 bone density classes (D1- D4) based on the clinical drilling resistance of the bone from oak or maple wood to styrofoam³¹. Norton and Gamble³² determined HU from computed tomography(CT) using bone morphology of Lekholm and Zarb classification. The study showed that for Q1 bone, HU was more than 850, for Q2-Q3 the HU was between 500-850, and for Q4 the HU was between 0-500. Trisi and Rao³³ determined Misch classification (D1-D4) related with histologic bone density determinations. This study found bone density to be 76.54±16.19% in D1, 66.78±15.82% in D2, 59.61±19.55% in D3 and 28.28±12.02% in D4 bone, but the bone scoring during drilling was based on tactile perception and, therefore, could not be classified, especially for D2 and D3 bone. The bone quality classifications were summarized in Table 1.

Table 1: Comparison of characterized bone with the bone quality classifications.

Lekholm&Zarb (1985) ³⁴		Trisi&Rao (1999) ³³ (%bone density)	Norton&Gambler (2001) ³² HU value	Misch (1998) ³⁵ Tactile analog	Rebaldi et al(2010) ²⁹ Hard-Normal-Soft	Typical Anatomy Location
Q1: Almost all of the jaw bone is comprised of homogenous compact bone		76.54±16.19%	>850	Dense cortical (D1) Oak or Maple	Q1 = hard bone	Anterior mandible
Q2: Thick layer of compact bone surrounds a core of dense trabecular bone		66.78±15.82%	500-850	Porous cortical and coarse trabecular (D2) White pine or Spruce		Anterior mandible Posterior mandible Anterior maxilla
Q3: Thin layer of cortical bone surrounds a core of dense trabecular bone		59.61±19.55%		Thin Porous cortical and fine trabecular (D3) Balsa wood	Q2 – Q3= normal bone	Anterior maxilla Posterior maxilla Posterior mandible
Q4: Thin layer of cortical bone surrounds a core of low-density trabecular bone		28.28±12.02%	0-500	Fine trabecular (D4) Styrofoam	Q4 = soft bone	Posterior maxilla

Bone quality and dental implant

Bone quality is an important factor for the success of dental implants because it affects the implant stability^{36,37}. Recent studies showed that the density of bone affected implant success, with a reduction in the density increasing the risk of failure^{2, 38} as shown in Figure 1. Previous studies indicated that implant surgical failure ranged from 3.2-5% in good-quality bone and 1.9-20% in poor bone quality, with most reports indicating greater failure rates (up to 65%) in soft bone³⁹.

There are differences in bone morphology between the maxilla and mandible. The mandible comprises a more compact bone than the maxilla and the maxilla is a more spongy bone than the mandible⁴⁰. Turkyilmaz and coworker reported that the bone quality around the implant in the mandible is more superior than in the maxilla⁴¹. It has been indicated that poor bone quality is the main risk factor for failure of implants, which also then associated with the implant stability and healing process^{42, 43}.

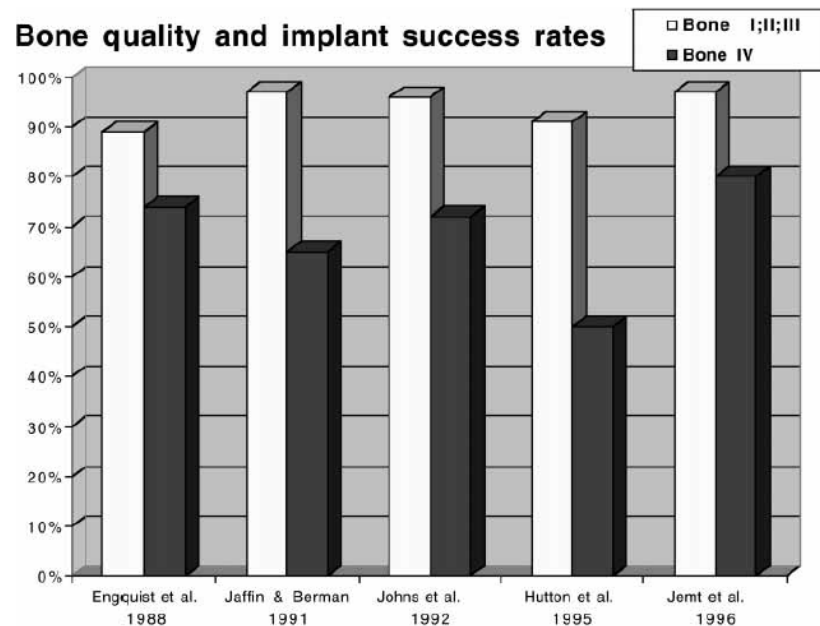


Figure 2: Implant success rates as related to bone quality³⁸

Cortical bone thickness

Cortical bone comprises mainly of hydroxyapatite crystallites and well-organized collagen fibrils, which causes the cortical bone to achieve a remarkable mechanical performance of high stiffness and toughness. Cortical bone thickness is one of the factors for a high implant success rate. More cortical thickness could increase the primary stability of the implant⁴⁴. Moreover, there are correlations between the cortical bone thickness with many factors relating to a bone density such as the Hounsfield Unit (HU) value from CT_s⁴⁵ and the insertion torque of implants⁴⁶. Many studies also indicated that the thickness of cortical bone directly influences implant success rates^{46 47}.

Evaluation of bone quality for dental implant placement

Many techniques were developed and used to evaluate the bone quality at dental implant installation sites, which were indicated by the primary stability of the dental implant. The resonance frequency analysis (RFA) mobility test, measurement of the insertion, and removal of torque value are the techniques usually performed to evaluate the primary stability. However, all of these techniques must be performed after the insertion of the dental implants. The measurement of the removal torque value, in particular, is an objective method, but its clinical application is difficult because it is irreversible and invasive method⁴⁸.

With the development of radiographic technology, the characteristics of bone and surrounding vital organs can be achieved prior to the dental implant placement. Preoperative radiographic examinations indicate some essential information including the mesio-distal, bucco-lingual and superior-inferior dimensions, the trabecular bone density and the cortical bone thickness. Preoperative implant imaging aims to acquire necessary surgical and prosthetic information to determine the quantity, quality and angulation of a bone, the selection of the potential implant sites, and to verify the absence of pathology.

Periapical radiograph.

A periapical radiograph is the first-choice diagnostic clinical instrument in dentistry⁴⁹. This method is practical, reliable and a non-invasive technique to evaluate the bone at the dental implant site^{50, 51}. However, this method has relatively low sensitivity, but there is high accuracy in detecting trabecular bone at the dental implant site⁵². Periapical radiographs assess the

bone quality using optical density by standard densitometry (Figure 4). For optical density, the film is scanned, and then the digital images are analyzed using computer software. The optical density of the interesting area is evaluated through densitometry variations of gray value, which vary from transparent to opaque (0 -255)⁵³. However, there are limitations in conventional periapical films such as errors in processing, increased radiation dosage, poor imaging geometry, lack of post-imaging facilities⁵³, non-reproducible imaging geometry, and distortions that are inherent to periapical radiography⁵⁴. The limitations for bone quality evaluation are image magnification and possible distortion, the limit value for determination of bone density and mineralization, and evaluation for 3D⁵⁵. Although the nature of the 2D image can never provide information in the bucco-lingual direction⁵⁶, periapical radiographs are still beneficial for pre-implant assessment because of availability and cost.



Figure 3: A: Periapical radiograph and radiopaque material to localize the implant installation site.

B: Periapical radiograph after dental implant placement.

Orthopantomography (OPG)

OPG was introduced into the market in the early 1960s⁵⁷. The technique produces a single radiographic image that includes both the maxillary and mandibular arches with supporting structures. OPG has been used for pre-implant evaluation and the preparation of treatment protocols. Although the resolution and sharpness of a panoramic radiograph are less than an intraoral radiograph, OPG is an excellent tool for the overview of the maxillofacial area, including many of the vital structures such as the maxillary sinus and inferior alveolar nerve (Figure 4).

OPG units are widely available, making this imaging technique very useful for screening⁵. However, the Information acquired from OPG should be used cautiously because this

technique has the significant limitations that are distortion (10% vertical magnification and 20% horizontal magnification) and error by patient position⁵⁸, the lack of image sharpness and resolution. This limitation leads to inaccurate interpretation⁴. Due to lack of image sharpness, lower resolution than periapical radiographs and image distortion, OPG should be used with caution for bone quality measurement.

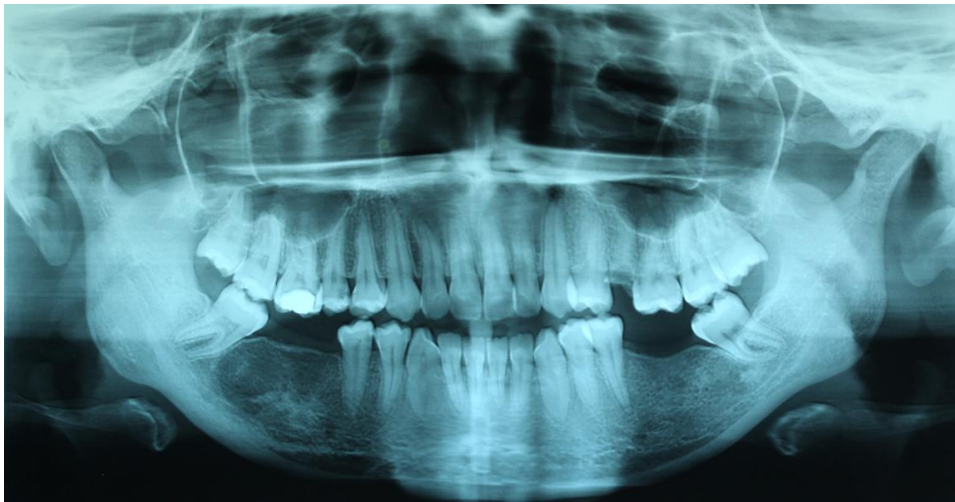


Figure 4: Orthopantomography (OPG) represents the maxillofacial area such as the maxilla and mandibular arch, the maxillary sinus and the inferior alveolar nerve

Cone-beam computed tomography (CBCT)

CBCT systems were developed in the 1990s. In 2001, CBCT was introduced as a 3D imaging modality. Since then it has largely replaced both single and multislice CTs for diagnostic imaging in oral implants⁵⁶. CBCT offers a radiographic method for the structural and qualitative analysis of the bone¹⁰⁻¹². Computer tomography (CT) software programs facilitate the measurement of the bone density by HU that is determined by the software programs in the CT machines, ranging from -1000 (air) to 3000 (enamel). The density of structures within the image is absolute and quantitative so it can be used to differentiate tissues in the region (i.e., muscle, 35–70 HU; fibrous tissue, 60–90 HU, cartilage, 80–130 HU; bone 150–1800 HU) and characterize bone quality (for D1 >1250 HU, for D2 850–1250 HU, for D3 350–850 HU, for D4 150–350 HU, and for D5 <150 HU)⁵⁹. CBCT is very sensitive to movement because of its very high spatial resolution. It has the following limitations: a limited contrast resolution that makes it less suitable for imaging soft tissues⁶⁰, high costs, and has a high radiation dosage absorbed by the patients or specimens.

The 2D measurement error of CBCT was found to range from 1.86-4.61% with no significant difference between the measurements and actual specimens⁶¹. To determine the length between CBCT and Micro-CT or actual specimens, Mangione and coworker⁶² found that the specimen always show a mathematical difference of about 0.2 mm. Baumgaertel and coworker⁶³ found that CBCT showed validity for measuring the length from a specimen compared with a caliper.

The gray density value from a CBCT can investigate the relationship with HU from CT. From the previous studies, a strong correlation was found between the gray density value of CBCT and the HU of CT^{64,65}. The gray density value from a CBCT is suggested to be used as the tool for evaluating the bone density^{66,67} (Figure 5). Several studies reported high geometric accuracy of CBCT for linear measurements^{13,15,68}, while its reliability in bone quality evaluation remains controversial. Only a few studies have suggested that CBCT could be applied to assess the trabecular bone microstructure^{14,69}. Nevertheless, CBCT does not represent calibrated voxel gray density value expressed in HU¹⁶. Many studies have been conducted to convert CBCT gray density value to actual density measurements¹⁷. The high correlation between the HU derived from CBCT voxel gray density value has been demonstrated, hinting at the potential for CBCT use in bone density assessment⁷⁰⁻⁷². The applications of CBCT in evaluating bone quality are still restricted for bone density assessment in some studies⁷³⁻⁷⁵. This may be due to the insufficient resolution of CBCT systems. The visibility of small anatomical structures with CBCT is largely influenced by the field of view (FOV), type of the CBCT system, setting selection, patient positioning, soft tissue thickness, voxel size and resolutions^{49,76}.

At the present, the studies showed the validity from CBCT data in 2D but in the bone density measurement, it is still controversial.

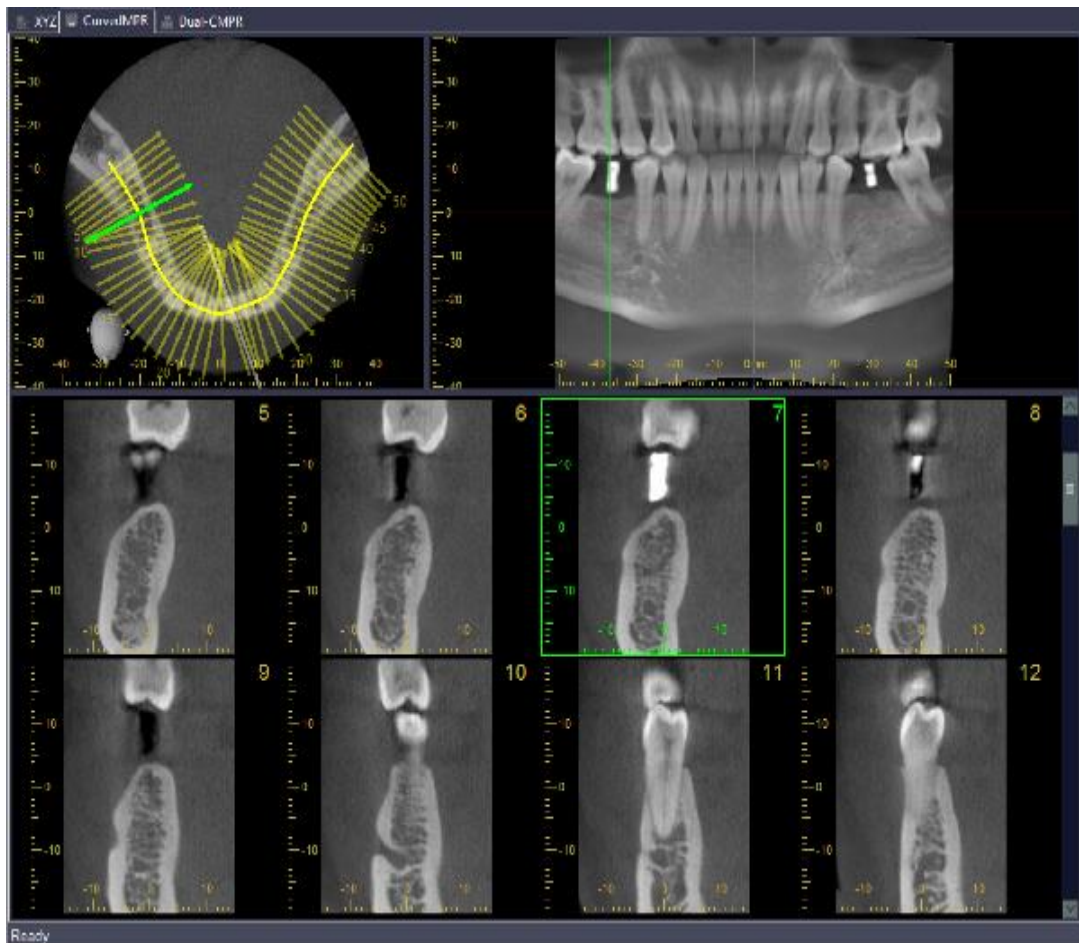


Figure 5: The bone density measurement from CBCT in grayscale at the implant site

Micro-Computed Tomography (Micro-CT)

The possibility of using a Micro-CT for noninvasive measurement of the bone–implant contact was first suggested by Feldkamp and coworker⁷⁷. A Micro-CT allows an assessment of the bone microarchitecture in 3D. This technique has achieved widespread use in the laboratory as a rapid, nondestructive method for specimens^{12, 78, 79}, animal models,^{80, 81} and allows for a full 3D reconstruction of the specimen (Figure 6). It is based on the same physical and mathematical principles with CBCT but the big advantage of Micro-CT is that it can acquire much higher resolutions (up to 10 μm)⁸².

Micro-CT uses data from multiple-angled attenuated X-ray projections to reconstruct a 3D representation of the specimen, which characterizes the spatial distribution of the material density. Micro-CT uses x-ray images to create cross-sections of a 3D-object that can be used to recreate models without destroying the original specimen⁸³. No specimen preparation is

required and testing is nondestructive. The resolutions of locally available Micro-CT systems are in the order of 6–72 μm for nominal isotropic substances, depending on the size and density of the sample⁸⁴. The Micro-CT data can be used to calculate histologic parameters⁸⁵ including bone volume (BV), bone surface (BS), trabecular separation (Tb.Sp), mean trabecular thickness (Tb.Th) and trabecular numbers (Tb.N) as well as nonmetric parameters like a structure model index (SMI), and connective density (Conn.D) for shape. Many studies showed a high correlation between Micro-CT and histologic analysis^{83,86,87}. These parameters describing the microarchitecture of bone have been shown to be important. Micro-CT is recommended as the gold standard for imaging of bone specimens studies at implant sites⁴⁹.

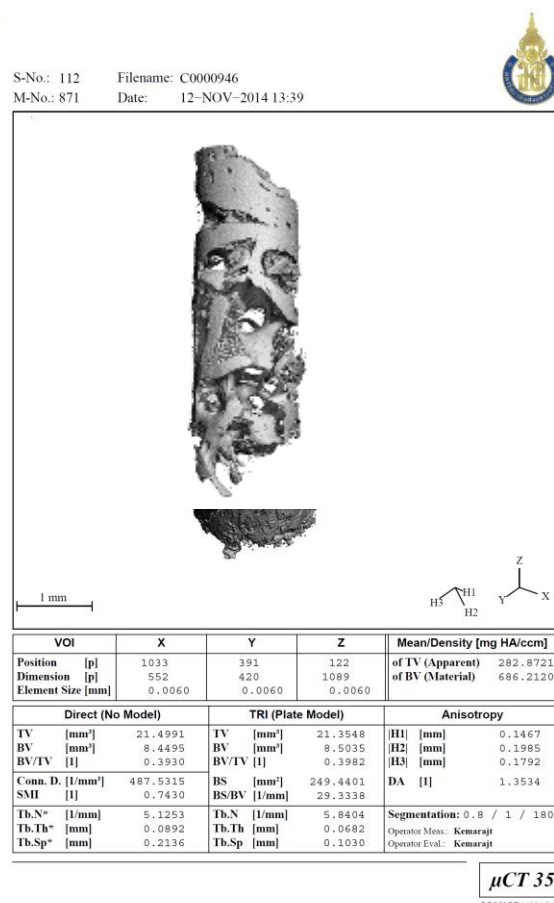


Figure 6: Micro- CT evaluation with the 3D reconstruction of a specimen for bone quality assessment

2. Histologic analysis

Histologic analysis is a subject normally considered in descriptive terms but sometimes it can be measured quantitative value⁸⁸. The measurements are made on 2D images, yet the information derived may be interpreted on a 3D basis. Results are usually showed in ratios or percentages (Figure 7). Although histologic analysis has been the gold standard for the morphometric examination of the bone specimen, however, the harvest of the bone specimen is invasive, destructive and requires a special preparation. Moreover, the structural properties for a specific location cannot be reassessed⁸⁹, only limited data sets can be obtained from serial sections,^{90,91} and the destructive nature of the procedure prevents the specimen from being used for further experiments.

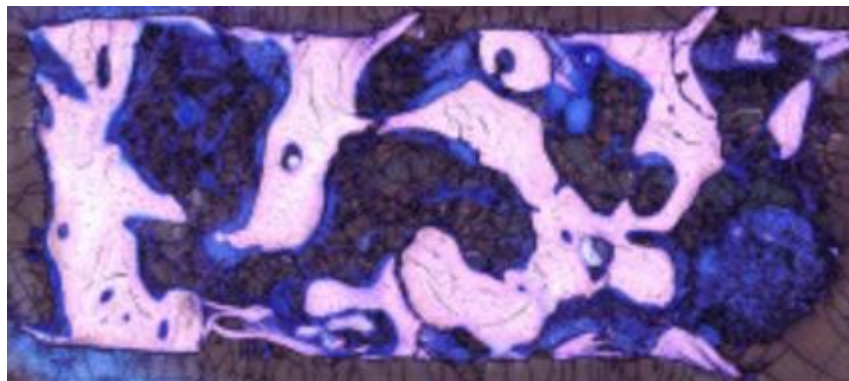


Figure 7: Histologic analysis for bone density measurement

The correlation of radiographic analysis for the bone quality assessment was summarized in Table2. Nevertheless, there are variations in subjective bone classification. The need for the measurement is very important because quantitative classification of bone density should be applied for pre-implant surgery that is not dependent upon operator experience³².

It is, therefore, important to determine the correlation of the periapical radiograph, CBCT radiographic and Micro-CT radiographic against histological analysis; the gold standard. The data of bone quality before implant placement is beneficial for implant planning and implant success rate prediction.

Table 2: The correlation of various techniques for bone morphology assessment.

Comparison	Results	Authors
Periapical radiograph vs CBCT	CBCT was statistically significantly better in terms of sensitivity (54%), positive (82.6%) /negative (44.5%) predictive values, and diagnostic accuracy (61%) when compared with digital radiographs (23%, 60%, 31%, 39%).	Stavropoulos A. and Wenzel A., 2007. ⁹²
	Periapical bone defects measured on periapical radiographs were approximately 10% smaller than on CBCT images.	Christiansen R. et al, 2009. ⁹³
	Periapical films are not reliable in the determination of the exact relationship between the apex of the tooth root and the maxillary sinus floor, compared with CBCT.	Hassan B.A. et al, 2010. ⁹⁴
	The periapical lesion was better detected by CBCT compared to periapical film. The positive and negative predictive values and accuracy for CBCT were all 1, compared with 1, 0.64 and 0.79 for periapical radiograph.	Liang Y.H. et al, 2014. ⁹⁵
Periapical radiograph vs histologic analysis	There was no correlation between the periapical radiograph and histological analysis from periapical pathology	Filho M.T. et al, 2009. ⁹⁶
	Periapical radiograph showed weaker correlations ($r = 0.5$, $P < 0.01$) with histologic analysis in bone density assessment	Corpas L. et al, 2011. ⁶⁹

Table 2: (Continued)

Comparison	Results	Authors
Periapical radiograph vs Micro-CT	Periapical films showed a specificity of 78% and a sensitivity of 44%. Apical root resorption may be underestimated when evaluated using digitized periapical radiographs compared with Micro-CTs.	Dudic A. et al, 2008. ⁹⁷
	A high correlation was found between periapical radiographs and Micro-CT in the assessment of trabecular bone.	Amouriq Y. et al, 2010. ⁹⁸
CBCT vs CT	CBCT-based gray density shows significantly higher values than CT-based values	Arisan V. et al, 2013. ⁹⁹
	Cone beam computed tomography (CBCT) and Micro-CT analyses were comparatively performed in maxillary sinus augmentation to preliminarily verify the diagnostic potential of CBCT on the evaluation of bone regeneration. Data were not statistically different between CBCT and Micro-CT , significant correlation between gray level(GL) and mineralized material amount(MM)	Soardi C. et al, 2012. ¹⁰⁰
	Strong correlation between grayscale of CBCT and Hounsfield units (HUs) of the CT scan	Razi T. et al, 2014. ⁶⁴
	To assess trabecular bone structure parameters (BV/TV, BS/BV, Tb.Th., and Tb.Sp.) from synthetic bone specimens of varying densities. The absolute values of the experimental results obtained using dental CBCT significantly differed from those obtained using Micro-CT. However, the results yielded by the	Ho J. T. et al., 2013. ¹⁰¹

Table 2: (Continued)

Comparison	Results	Authors
CBCT vs CT	two instruments demonstrated a strong positive correlation ($r= 0.9296$ ($p < .001$), 0.8061 ($p < .001$), 0.9390 ($p < .001$), and 0.9583 ($p < .001$), respectively.	
	Trabecular bone microstructural measurements varied significantly, especially in smaller fields of view. There was no significant difference in the trabecular parameters when using different resolutions.	Ibrahim N. et al, 2013. ⁴⁹
	Grey value in CBCT systems significantly deviated from Hounsfield unit values measured with MSCT ($p = 0.0001$). Grey-level values from CBCT images are influenced by device and scanning settings.	Parsa A. et al, 2013. ¹⁰²
	There was a linear relation between the grey levels and the attenuation coefficients. This made it possible to calculate Hounsfield units from the measured grey levels.	Reeves T.E. et al, 2012 ⁶⁵ .
CBCT vs	No association found between CBCT and bone density from histological analysis.	Livada R. et al, 2009. ¹⁰³
Histologic analysis	The bone density measured by both histologic analysis of bone biopsies and the CBCT analysis of bone density expressed in Hounsfield units were compared. There was a statistical significant correlation between radiographic and histologic analysis.	Leavitt C.H. et al, 2010. ¹⁰⁴

Table 2: (Continued)

Comparison	Results	Authors
<p>CBCT vs Histologic analysis</p>	<p>CBCT imager, with a spatial resolution as high as 80 μm, had significant correlations with histologic analysis on decalcified bone specimens for <i>ex vivo</i> quantification of peri-implant trabecular microstructure.</p>	<p>Huang Y. et al, 2014.¹⁰⁵</p>
	<p>Histologic data demonstrate a definite correlation with the formation of new, vital autogenous trabecular bone and bone mineral density from CBCT.</p>	<p>Lee C. et al, 2011.¹⁰⁶</p>
<p>CBCT vs Micro-CT</p>	<p>There were a relation between bone density obtained by CBCT (RBD) and morphometric parameter of bone analyzed by Micro-CT. Positive correlations between BV/TV ($r = 0.769$, $P < 0.001$), BS/TV ($r = 0.563$, $P = 0.002$), Tb.Th ($r = 0.491$, $P = 0.009$), Tb.N ($r = 0.518$, $P = 0.005$) and BMD ($r = 0.699$, $P < 0.001$) with RBD were identified. On the contrary, BS/BV ($r = -0.509$, $P = 0.006$), Tb.Sp ($r = -0.539$, $P = 0.003$) and Tb.Pf ($r = -0.636$, $P < 0.001$) were negatively correlated with RBD.</p>	<p>Monje A. et al, 2014.¹⁰⁷</p>
	<p>There were difference measurement in bone volume fraction (BV/TV) and trabecular thickness (Tb.Th.) using CBCT and Micro-CT. However, the parameters showed correlation between CBCT and Micro-CT.</p>	<p>Ho J. T. et al., 2013.¹⁰¹</p>

Table 2: (Continued)

Comparison	Results	Authors
CBCT vs Micro-CT	There were a high correlations between the grayscale measured using CBCT and the trabecular bone microarchitecture parameters (BV/TV and TbTh) measured using Micro-CT, in addition to high correlations between the cortical bone morphology measured using Micro-CT and dental CT.	Hsu J.T. et al, 2014. ¹⁰⁸
Micro-CT and Histologic analysis	The bone configuration in the Micro-CT images corresponded to that observed in the histologic sections. The correlation between Micro-CT and histology was significant for cortical ($r = 0.65$; $P < .05$) and cancellous bone ($r = 0.92$; $P < .05$)	Butz, F. et al, 2006. ¹⁰⁹
	Good correlation between cortical bone structural measured obtained from Micro-CT datasets and from two-dimensional histological sections.	Particelli, F. et al, 2012. ⁸⁷
	Biopsy bone core were harvested from posterior maxilla. The relationship between bone density obtained by histologic analysis and morphometric parameter of bone by Micro-CT was analyzed. Significant positive correlations were observed between BV/TV from Micro-CT and the percentage of bone from histologic analysis.	Garcia, R., et al, 2013 ⁸³

Table 2: (Continued)

Comparison	Results	Authors
Micro-CT and Histologic analysis	Bone implant contact (BIC) and bone implant volume (BIV) obtained from histologic analysis showed no significant difference with those obtained from Micro-CT scan.	Bernhardt R. et al, 2012 ⁸⁶
	Bone implant contact (BIC) assessed in histological image (mean: 61.77±17.07%, median: 64.80%) and Micro-CT (mean: 59.50±16.93%, median: 59.50%) showed a positive correlation (r= 0.854).	Becker, K. et al, 2015. ¹¹⁰

Objective of the study**Primary Objective**

To determine the correlation between periapical radiography, CBCT, Micro-CT and histologic analysis in the assessment of the bone quality of jaw bones for dental implant placement.

Secondary Objectives

To evaluate the bone morphology in maxilla and mandible.

To propose a pre-operative parameter for predicting the bone quality for dental implant placement from periapical radiograph or CBCT using the correlation data from Micro-CT and histologic analysis.

Expected outcome

To provide scientific knowledge of the correlation between a conventional periapical radiograph, CBCT, Micro-CT and histologic analysis for assessment bone quality of jaw bones.

A parameter from periapical radiograph or CBCT that shows a strong correlation with bone density parameters from Micro-CT or histology assessment will benefit the clinician to predict the quality of bone at the implanted site prior the implant installation procedure.

Hypothesis

There is a correlation between the gray value from the periapical radiograph, gray density value from CBCT, and bone density parameter (BMD, BV/TV and %porosity) from Micro-CT and % bone from histologic analysis.

CHAPTER 2

MATERIALS AND METHODS

Patients

The study protocols were approved by the Human Research Ethics Committee, Faculty of dentistry, Prince of Songkla University (Code No. EC5509-35-P).

Patients requiring dental implant placements were included in the study. Subjects considered eligible for the study included those 20 years or older and physically healthy, with no underlying systemic diseases, as determined by medical history records. Patients who had an alveolar height of less than 10 mm, needing immediate/delay-immediate implant placements or needing small diameter (less than 3 mm) implant placements were excluded.

All patients had a tooth extracted at least 6 months prior to implant surgery. The implant therapy was planned based on the radiographic and clinical evaluation.

Bone samples were grouped according to the region of harvesting: UA (upper anterior), UP (upper posterior), LA (lower anterior), and LP (lower posterior). Samples from each group were collected and analyzed according to the protocol.

The sample size calculation, from one way ANOVA, α was set at 0.05, 80% power of test. The samples were studied at least 9 per each groups⁹⁶.

Methodology

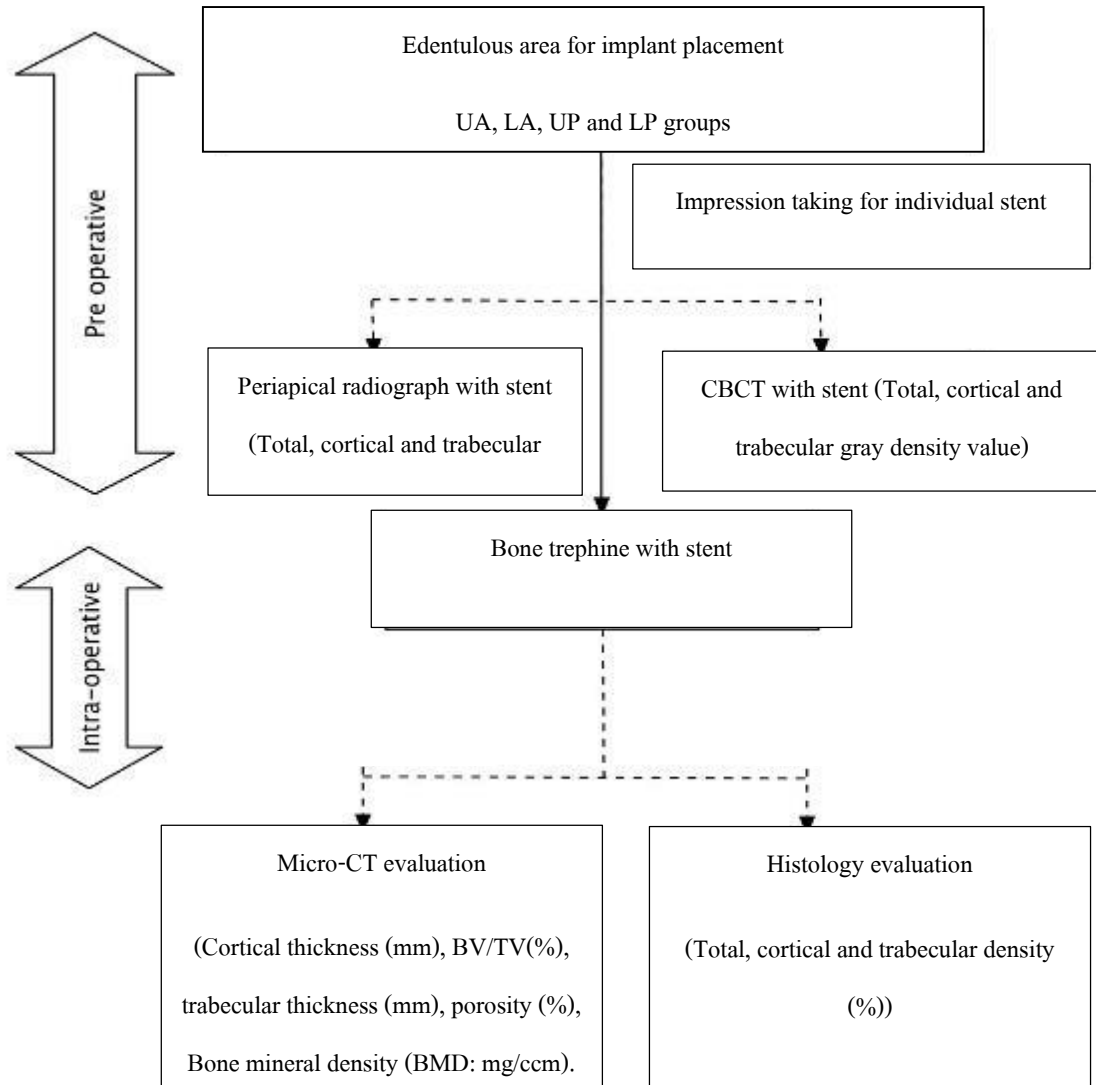


Figure 8: The conceptual framework of the experimental design

Pre-operative protocol

The radiographic stents with radiopaque markers located at the surgical site were prepared in a cylindrical shape and used during the periapical radiography and CBCT (Figure 9)

**9A****9B**

Figure 9: (9A) Study cast for radiographic stent construction. (9B) Radiographic stent with radiopaque markers for locating bone quality measurement

Conventional periapical radiography procedure

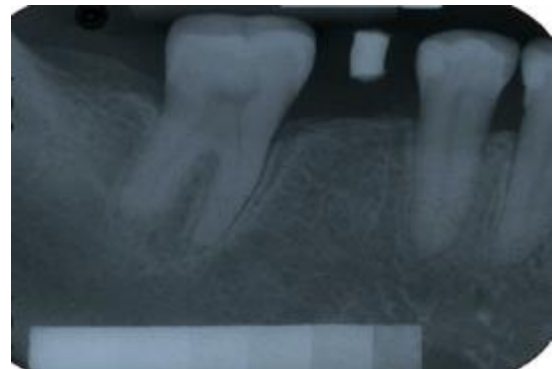
Standardized periapical radiographs of the experimented sites were taken (10mA, 65 KVP, 0.42s 12 in FFD) using dental x-ray film size No.2 (Kodak, Ultra speed, USA) with a standardized custom lead step wedge. An X-ray machine was used (Gendex, IL, USA) and the films were processed by an automatic film processor (Dent X 9000, DentX/Logetronics GmbH, Germany). The films were transformed into digital TIFF files by a scanner (Epson: Perfection 4870 Photo, Seiko Epson Corp, Japan).

A custom lead step wedge preparation was arranged by using a lead strip from film No.2. The first stripe was cut 5 mm in width and 30 mm in length. The remaining 5 strips must be cut progressively 5 mm shorter in length but with the same width. The stripes were placed one on top of the other, starting with the longest and getting progressively smaller until a series of even steps were built up, then the strips were glued together and the films were sealed (Figure10)

The gray value was calculated from the corresponding area 2x2 mm (cortical bone area), 2x3 mm (trabecular bone area) and 2x5 mm (total bone area) for dental implant placements using Image J program V1.46r for gray value measurement (Figure 11).



10A



10B

Figure 10: (10A) Periapical radiograph with lead step wedge.

(10B) Radiographic stent with the parallel hole filled with radiopaque material to locate the position for bone density measurement

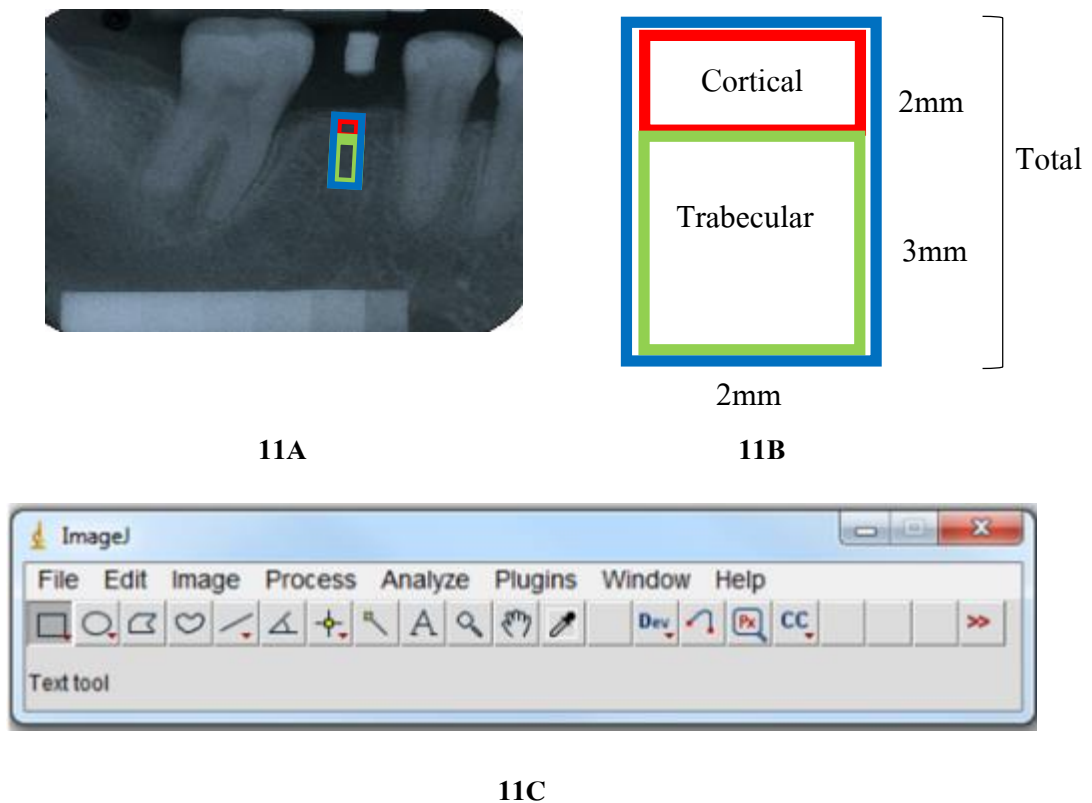


Figure 11: (11A) The periapical radiograph with area for gray value measurement
 (11B) Area for bone density measurement the cortical (2x2 mm), trabecular (2x3 mm) and total (2x5 mm) gray value measurement underneath radiopaque marker from periapical radiograph
 (11C) Image J program for gray value measurement from periapical radiograph

CBCT procedure and analysis

CBCT (3D Accuitomo, J. Morita, Japan) was used for preoperative evaluation of implanted site. The intended implant site was located by radiographic stent with a radiopaque marker (Figure 11). CBCT scan was performed under the following conditions: a tube current of 5 mA, a tube voltage of 90 kV, and a field of view (FOV) of 40 mm in diameter; with a voxel size of 0.125 mm; 17.5 seconds.

The corresponding area (2x5 mm) for dental implant placements were localized and analyzed for the gray density value at the voxel in the region of interest (ROI). (Figure12). The measurements were as follows: i) cortical thickness, ii) cortical gray density value (2x2 mm), iii) trabecular gray density value (2x3 mm), and iii) total gray density value (2x5 mm) using One volume viewer program V1.5.0 (2¹⁶ bit) for gray density value measurement.

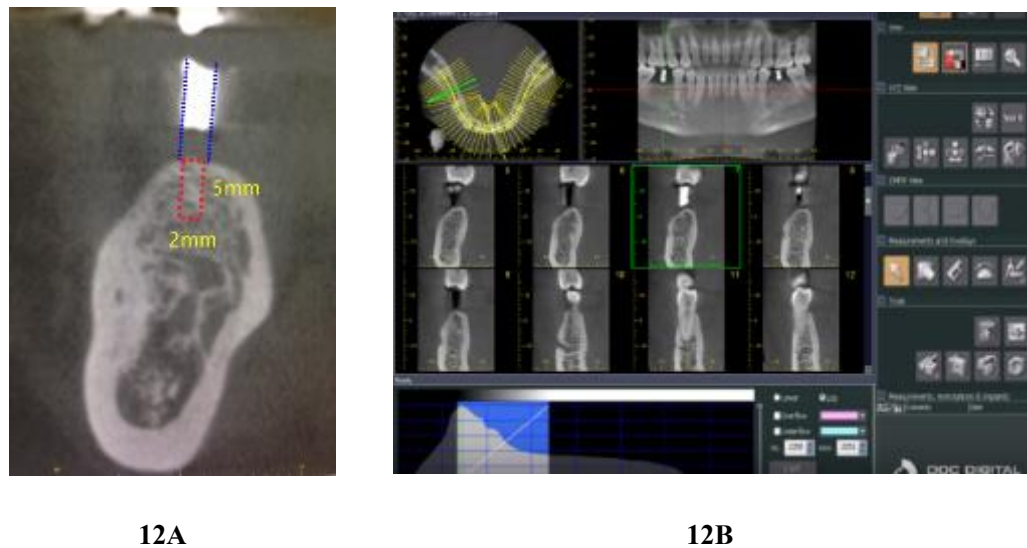


Figure 12: (12A) Radiographic stent with the parallel hole filled with radiopaque material to locate the position for bone density measurement.
 (12B) One volume viewer program for gray density measurement from CBCT

Bone trephine procedure

At the time of the implant placement, the radiographic stent was placed to locate the bone retrieval site. After the administration of local anesthesia (4% articaine hydrochloride (Ubistesin 1:200,000; 3M ESPE, Platz, Seefeld, Germany)), a midcrestal incision was performed and a mucoperiosteal flap was elevated to allow access to the alveolar ridge. The initial bone drill was performed with a 2x5 mm long trephine bur (TRE020M, Hu-Friedy Mfg Co LLC, Zweigniederlassung, Germany) through the radiographic stent. This allowed for a core of bone 2x5 mm long to be obtained. The implant site preparation was then completed, the implant was installed, and the flaps were approximated with a synthetic absorbable suture. After retrieval, each bone specimen was fixed and stored in 10% neutral-buffered formalin for Micro-CT and histologic analysis (Figure13).

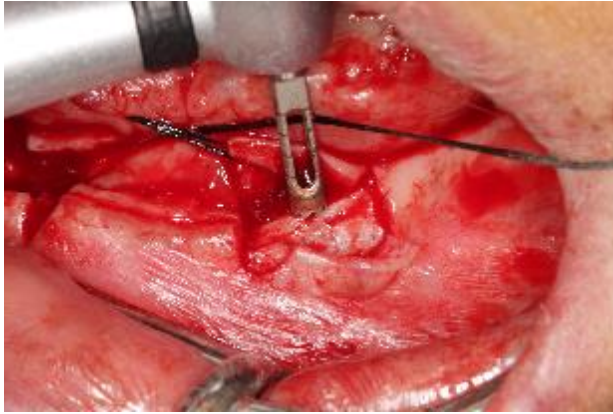
**13A****13B**

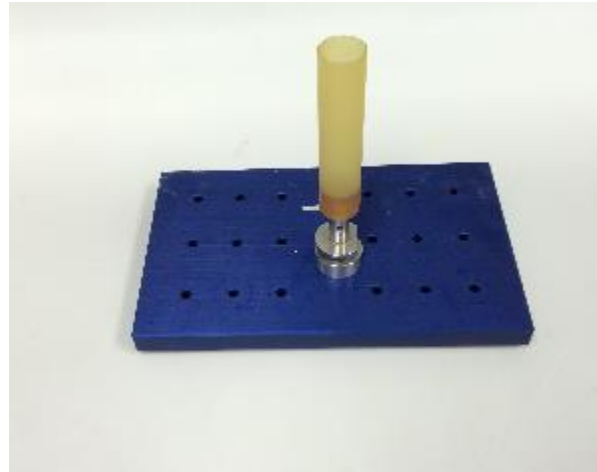
Figure 13: 13A and 13B Bone trephine for Micro-CT and histologic analysis

Micro-CT analysis

To obtain a high-resolution for quantitative measurement of bone formation, Micro-CT (Scanco 35, Switzerland) imaging was performed for each bone sample. Trephined and formalin-fixed bone cores placed in a sample holder 7 mm x 60 mm were used for Micro-CT analysis (70 kV 114uA). The specimens were analyzed to evaluate the cortical thickness (mm), bone volume fraction (BV/TV: %), trabecular thickness (Tb.Th: mm), porosity (%) and bone mineral density (BMD; mg/ccm) using Micro-CT 35 V. 4.1 program. (Figure14).



14A



14B



14C

Figure 14: (14A) Bone specimen from trephine bur.

(14B) The specimen's holder for Micro-CT scanning.

(14C) Micro-CT (Scanco 35, Scanco Medical AG, Switzerland)

Histologic preparation and assessment (Undecalcified bone specimen)

The specimens were dehydrated using ascending grades of alcohol, infiltrated and embedded in methylmethacrylate (MMA, Technovit 7200 NEU, Heraeus Kulzer, Wehrheim, Germany) for undecalcified sectioning (Figure15). After the specimens completely polymerized (Figure16), each specimen were cut along the long axis of the specimens, using a diamond

wire saw (Exakts, Apparatebau, Norderstedt, Germany) (Figure17). All specimens were glued with acrylic cement (Technovit 7210 VLC, Heraeus Kulzer) to silanized glass slides (Super Frost, Menzel GmbH, Braunschweig, Germany) and ground to a final thickness of approximately 40 μm . The slides were cleaned with alcohol –acetone 1:1, agitated for 5 minutes in 30% H_2O_2 , rinsed with water and then stained for 15 minutes with Toluidine blue, rinsed in water, dried slide and covered with slip¹¹¹ (Figure18) .



Figure 15: The specimens were dehydrated using ascending grades of alcohol, infiltrated and embedded in MMA



Figure16: The specimens were embedded in MMA and completed polymerization for undecalcified sectioning

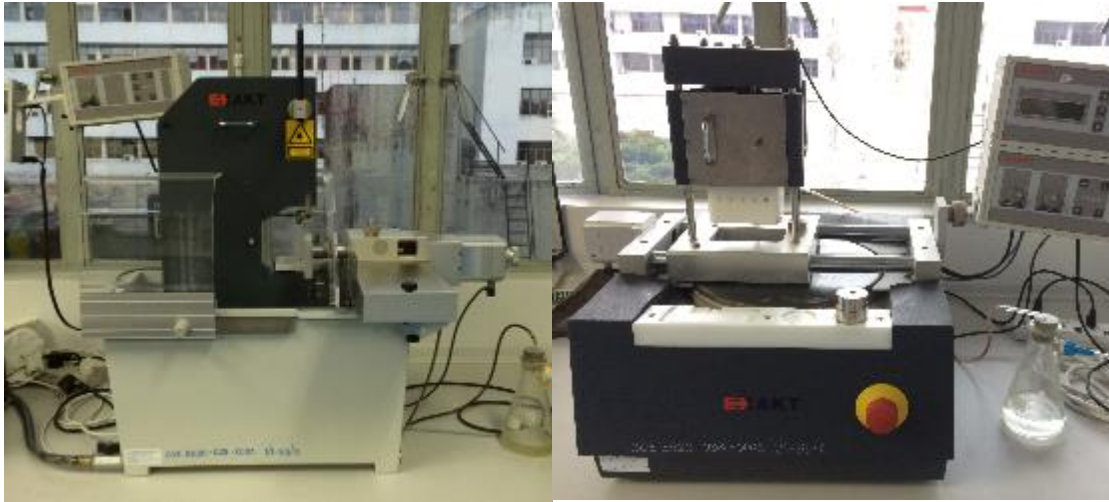


Figure17: The cutting and grinding machines for undecalcified sectioning

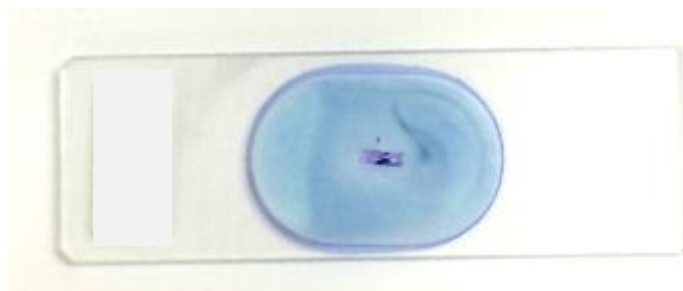


Figure18: The specimen was stained with toluidine blue

Histologic analysis

Histologic analysis was performed by images captured using a light microscope (Axiostar, Carl Zeiss, Germany) at the magnification of 5x, associated with a camera (Axiocam mRC, Carl Zeiss, Germany). Digital images were evaluated using the image analysis software program (Image Pro® Plus 7.0, Media Cybernetics, Silver Springs, MD, USA). The following parameters of the bone specimens were evaluated with the percentage of cortical, trabecular and total bone specimen (proportion of area of bone to total area) (Figure 19).

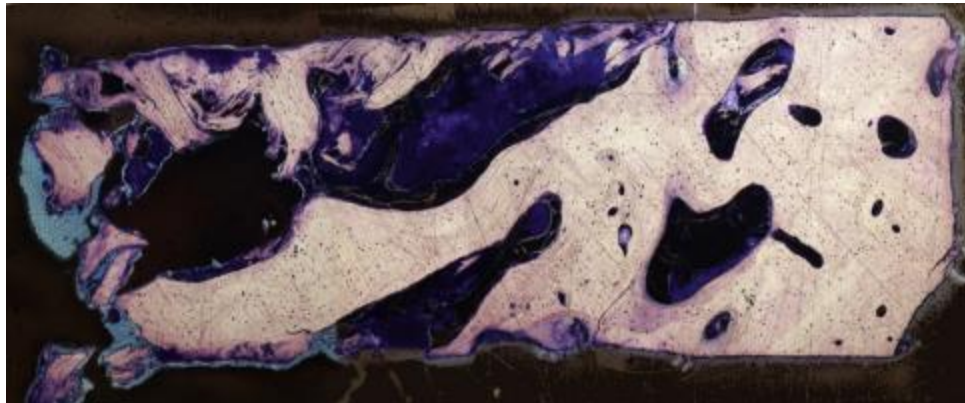


Figure19: Histologic preparation and stained with Toluidine blue for the measurement percentage area of cortex and trabecular bone

Statistical Analysis

Statistical analysis was performed using SPSS (V16, SPSS Inc., Chicago, IL, USA). Descriptive statistics were performed to characterize the bone morphology of 4 study groups. The cortical bone thickness and bone density parameters were reported using means and standard deviation. The normality test was conducted for parametric statistical analysis. One way ANOVA and Post hoc analyzes using Tukey HSD were applied to reveal statistically significant differences between 4 regions.

Pearson correlation coefficients and simple linear regression were used to estimate the relationship between corresponding parameters measured with different techniques and to examine the strength of a relationship between the cortical thickness measurement (CBCT) and bone density values (Micro-CT and histology). The level of statistical significance was set at $P < 0.05$.

To determine the reliability of the measurements, 62 randomly selected radiograph and histology slide were reexamined and remeasured at 1 months after the initial measurements. The intra-operator reliability was reported by calculating the intraclass correlation coefficient (ICC) between both measurements.

CHAPTER 3

RESULTS

A total of sixty-two bone cores were obtained from 31 maxilla and 31 mandible bone samples from 41 patients with a mean age of 54.71 years. Table 3 detailed 4 groups of the study according to gender (26 males, 36 females), age and location of the area (previously tooth number) where the specimens were obtained.

Table 3: Sample (n= 62) investigated in this study

Groups	Gender (Male/Female)	Mean age	Bone core location (number of samples)	Total sample size (n)
Upper Anterior (UA)	8/4	52.58 ± 15.79	11(2), 21 (1) 12(4), 22(3) 13(1), 23 (1)	12
Upper Posterior (UP)	8/11	55.05±12.11	14(3), 24(3) 15(1), 25(2) 16(3), 26(3) 17(2), 27(2)	19
Lower Anterior (LA)	4/6	56.60±20.33	31(1) 33(5) 43(4)	10
Lower Posterior (LP)	6/15	54.71±10.83	34(1) 35(3), 45(1) 36(6), 46(8) 37(1), 47(1)	21

Evaluation of bone morphology using a periapical radiograph, CBCT, Micro-CT and histologic analysis

Upper anterior (UA) region (Figure 20)

The bone core harvested from the anterior maxilla showed thin cortical bone with fine trabecular bone.

Periapical radiographs (figure 20a) displayed a fine trabecular pattern with an unidentified cortical bone region. The mean gray value was 94.39 ± 22.32 with the higher density in the lower part (gray value: 97.98 ± 19.25) compared to the upper part (gray value: 86.54 ± 19.96).

CBCT (figure 20b) showed very thin cortical bone thickness with moderated density of trabecular bone and fine trabecular bone pattern. The mean gray density value of CBCT from the cortical bone area (1997.63 ± 274.35) demonstrated higher density compared to the mean gray density value from the trabecular bone area (1902.77 ± 279.85). The total gray density value from the upper anterior region was 1943.68 ± 268.45 .

Micro-CT (figure 20c, 20d) showed moderate cortical bone thickness with a high density of trabecular bone. The measured parameters were as followed: BV/TV: 35.24 ± 10.68 %, trabecular thickness: 0.1516 ± 0.06 mm, porosity: 64.76 ± 10.68 % and BMD 356.72 ± 157.07 mg/ccm.

Histologic analysis (figure 20e) showed moderate cortical bone thickness with an average density of trabecular bone. Mean bone density from the cortical bone area (63.07 ± 11.03 %) was denser than the trabecular bone area (39.74 ± 10.30 %). The bone density value from the upper anterior region, measured using the histologic method, was 44.55 ± 9.98 %.

According to the cortical bone thickness of the UA region, the measurement could be done only using CBCT (1.01 ± 0.23 mm), Micro-CT (1.00 ± 0.25 mm) and histologic analysis (1.00 ± 0.27 mm).

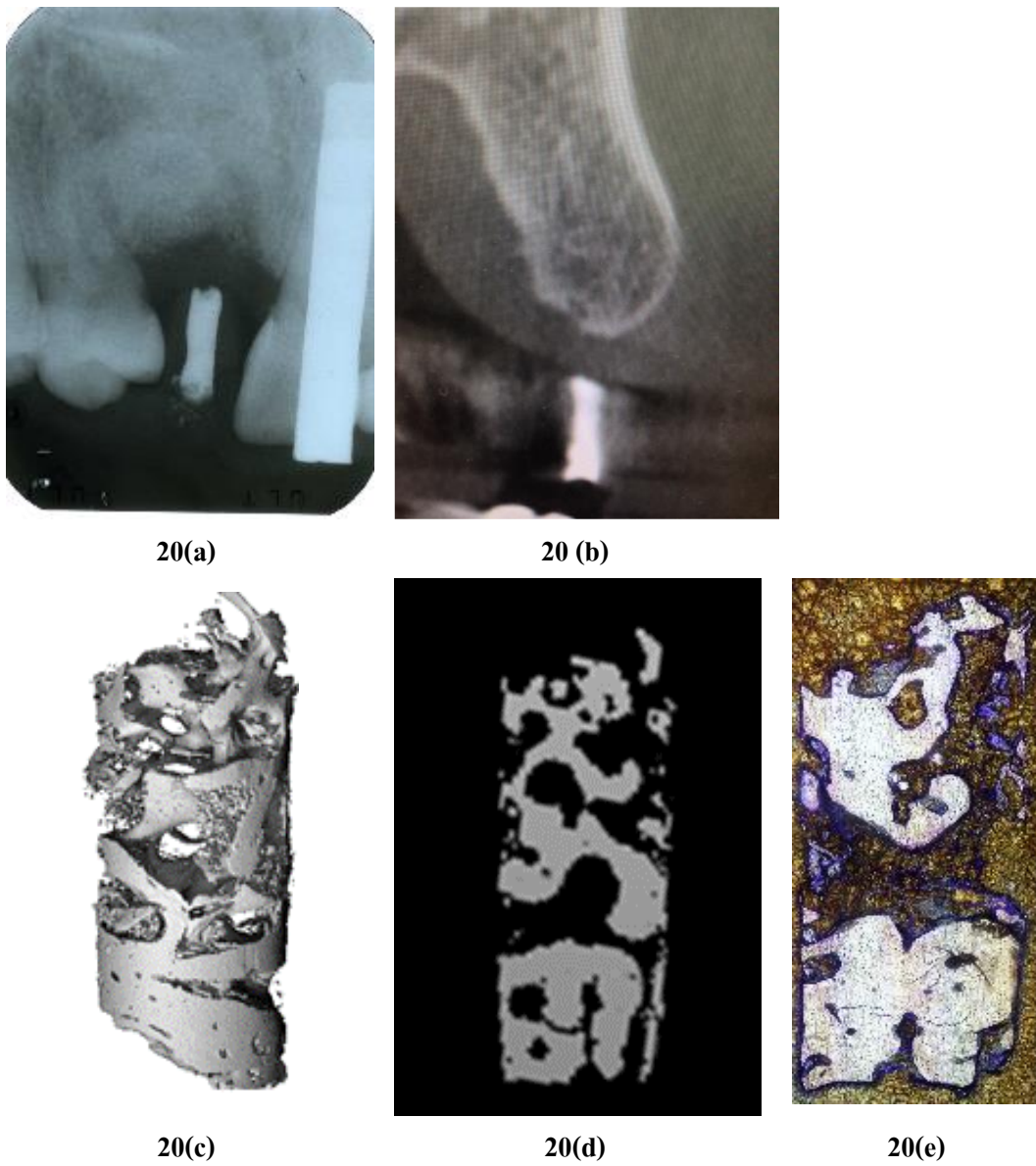


Figure 20 (a-e): The comparison of the image received from the periapical radiograph (20a), CBCT (20b), Micro-CT (20c, 20d) and histologic analysis (20e) from the upper anterior region (UA)

Upper posterior region (UP) (Figure 21)

The bone core from posterior maxilla presented very thin cortical with very thin trabecular bone.

Periapical radiographs (figure 21a) showed fine to coarse trabecular patterns with unidentified cortical bone. The mean gray value from the upper posterior region was 83.39 ± 20.22 with the higher density in the lower part (gray value: 90.01 ± 6.23) compared to the upper part (gray value: 77.85 ± 4.04).

CBCT (figure 21b) showed very thin cortical bone thickness with a low density of trabecular bone and a very fine trabecular bone pattern. The mean gray density value of CBCT from the cortical bone area (1842.70 ± 465.21) demonstrated higher density compared to the mean gray density value from the trabecular bone area (1733.47 ± 478.12). The total gray density value from the upper posterior region was 1784.66 ± 446.87 .

Micro-CT (figure 21c, 21d) showed thin cortical bone thickness with an average density of trabecular bone. The measured parameters were as followed: BV/TV: 36.11 ± 9.15 %, trabecular thickness: 0.1728 ± 0.06 mm, porosity 63.89 ± 0.15 % and BMD 341.46 ± 140.50 mg/ccm.

Histologic analysis (figure 21e) revealed thin cortical bone thickness with a low density of trabecular bone. Mean bone density from the cortical bone area (61.28 ± 7.56 %) was denser than the trabecular bone area (36.68 ± 11.72 %). The bone density value from the upper posterior region, measured using the histologic method, was 40.51 ± 11.54 %.

Measuring the cortical bone thickness of the UP region could only be conducted using a CBCT (0.87 ± 0.18 mm), Micro-CT (0.90 ± 0.18 mm) and histologic analysis (0.89 ± 0.16 mm).

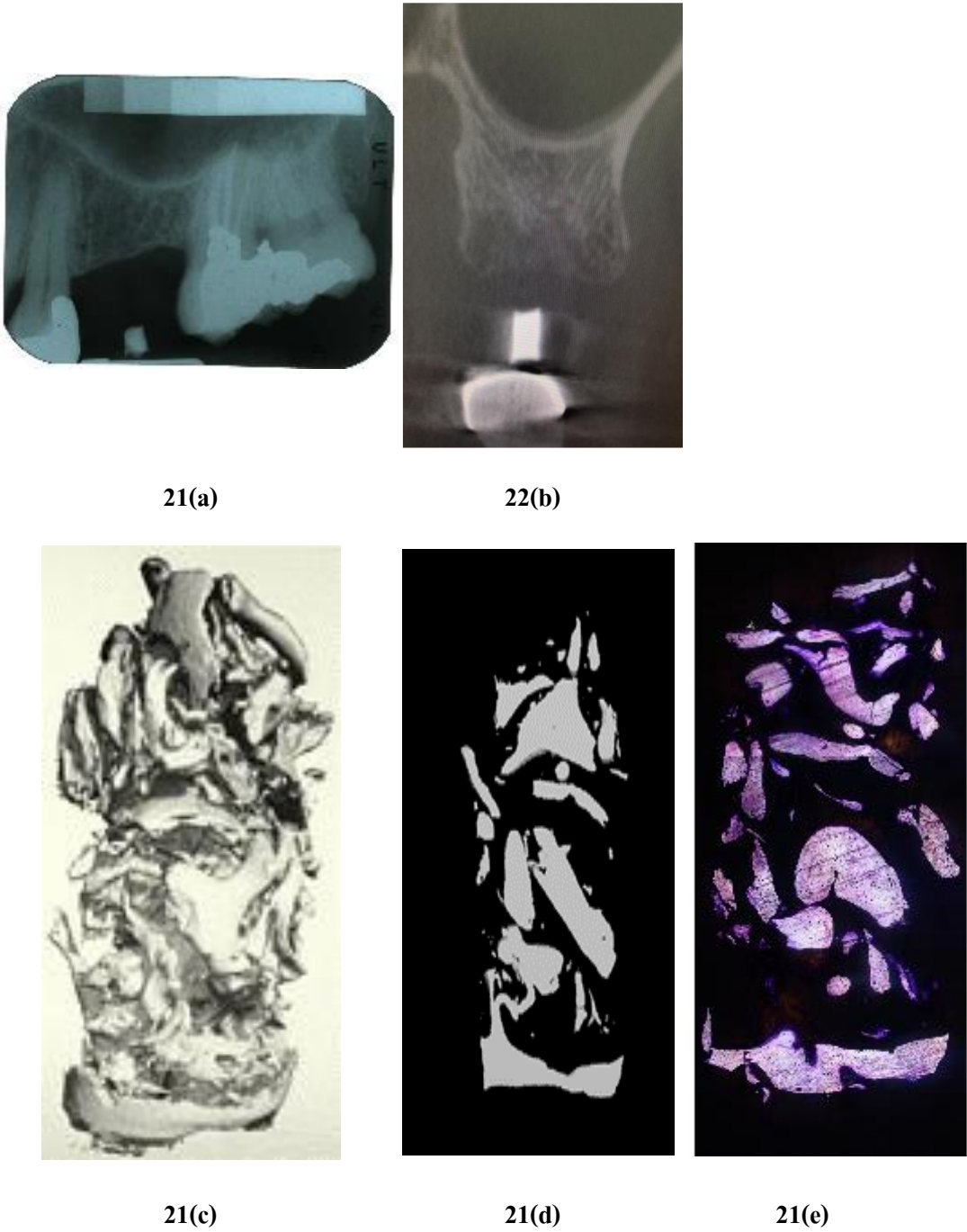


Figure 21 (a-e): The comparison of the image received from a periapical radiograph (21a), CBCT (21b), Micro-CT (21c, 21d) and histologic analysis (21e) from the upper posterior region (UP)

Lower anterior region (LA) (Figure 22)

The bone core from the anterior mandible displayed thick cortical bone with dense trabecular bone.

The periapical radiograph (figure 22a) showed a coarse trabecular pattern, however, the cortical bone could not be identified. The mean gray value from the lower anterior region was 117.88 ± 43.90 with the higher density in the lower part (gray value: 118.66 ± 17.27) compared to the upper part (gray value: 105.24 ± 18.39).

The CBCT (figure 22b) showed thick crestal cortical bone with a high density of trabecular bone and a coarse trabecular bone pattern. The mean gray density value of the CBCT from the cortical bone area (1856.89 ± 151.62) revealed higher density compared to the mean gray density value from the trabecular bone area (1674.97 ± 115.64). The total gray density value from the lower anterior region was 1769.07 ± 132.01 .

The Micro-CT (figure 22c, 22d) showed thick cortical bone with a high density of trabecular bone. The measured parameters were as followed: BV/TV: $63.25 \pm 19.86\%$, trabecular thickness: 0.2679 ± 0.09 mm, porosity $45.84 \pm 9.15\%$ and BMD 521.18 ± 210.71 mg/ccm.

Histologic analysis (figure 22e) showed thick cortical bone with a high density of trabecular bone. The mean bone density of the cortical bone area ($68.86 \pm 4.39\%$) was slightly denser than the trabecular bone area ($50.26 \pm 7.21\%$). The bone density value from the lower anterior region, measured using the histologic method, was $55.62 \pm 9.97\%$.

The measurement of the cortical bone thickness of the lower anterior region could only be conducted using a CBCT (1.19 ± 0.24 mm), Micro-CT (1.20 ± 0.22 mm) and histologic analysis (1.23 ± 0.20 mm).



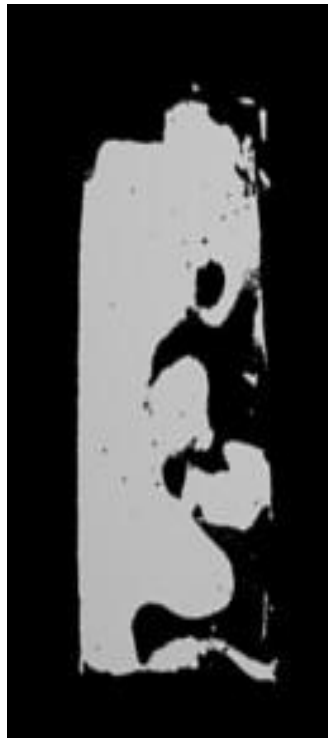
22(a)



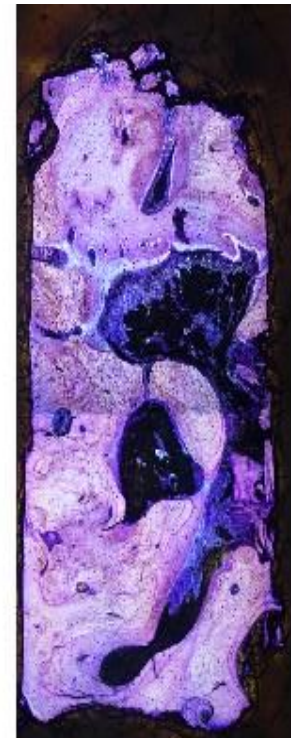
22(b)



22(c)



22(d)



22(c)

Figure 22 (a-d): The comparison of the image received from a periapical radiograph (22a), CBCT (22b), Micro-CT (22c) and histologic analysis (22d) from the lower anterior region (LA).

Lowerior region (LP) (Figure 23)

The bone core from the posterior mandible demonstrated thick cortical bone with dense trabecular bone.

The periapical radiograph (figure 23a) showed a coarse trabecular pattern. The mean gray value from the lower posterior region was 91.07 ± 32.61 with the higher density in the lower part (gray value: 93.41 ± 7.18) compared to the upper part (gray value: 83.18 ± 6.81).

The CBCT (figure 23b) showed thick crestal cortical bone with a high density of trabecular bone and a coarse trabecular bone pattern. The mean gray density value of CBCT from the cortical bone area (1930.40 ± 438.44) revealed higher density compared to the mean gray density value from the trabecular bone area (1787.16 ± 391.67). The total gray density value from the lower posterior region was 1848.49 ± 413.55 .

The Micro-CT (figure 23c, 23d) represented thick cortical bone thickness with a high density of trabecular bone. . The measured parameters were as followed: BV/TV: $46.74 \pm 13.14\%$, trabecular thickness: $0.2384 \pm 0.07\text{mm}$, porosity $53.25 \pm 13.14\%$ and BMD $480.76 \pm 186.21\text{ mg/ccm}$.

Histologic analysis (figure 23e) showed thick cortical bone with a high density of trabecular bone. Mean bone density from the cortical bone area ($66.64 \pm 11.33\%$) was denser than the trabecular bone area ($44.58 \pm 9.95\%$). The bone density value from the lower posterior region, measured using the histologic method, was $51.61 \pm 13.07\%$.

The measurement of the cortical bone thickness of the lower posterior region could only be conducted using a CBCT ($1.16 \pm 0.25\text{mm}$), Micro-CT ($1.17 \pm 0.25\text{mm}$) and histologic analysis ($1.17 \pm 0.23\text{mm}$).

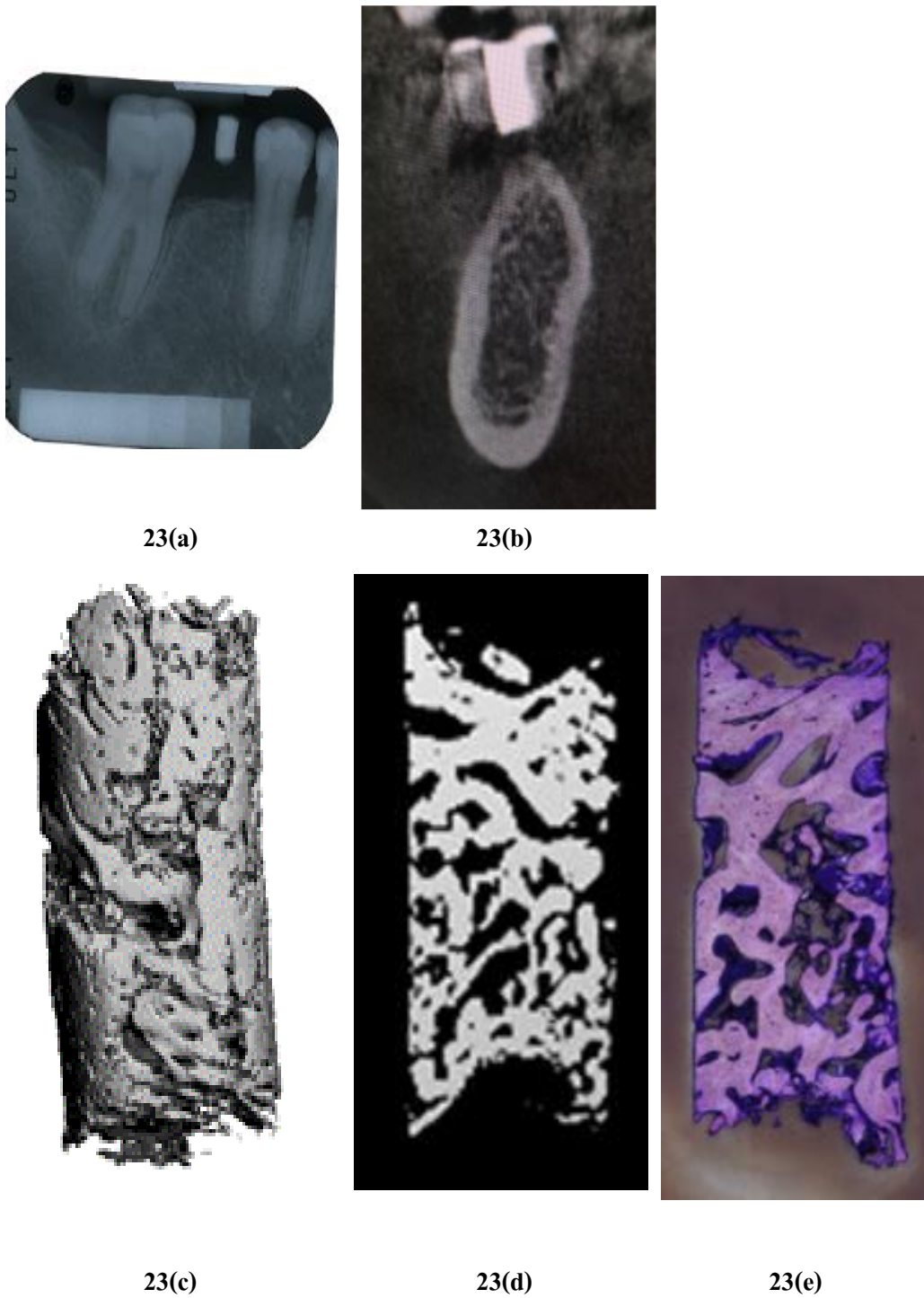


Figure 23 (a-d): The comparison of the image received from a periapical radiograph (23a), CBCT (23b), Micro-CT (23c, 23d) and histologic analysis (23e) from the lower lower posterior region (LP).

The correlation among periapical radiograph, CBCT, Micro-CT and histology analysis in the assessment of bone quality

The parameters for bone density from a periapical radiograph (gray value), CBCT (gray density value), Micro-CT (BV/TV, trabecular thickness, porosity, BMD), and histologic analysis (bone density), measured from 4 regions, were summarized in Table 4 and Figure 24-32.

Table 4: The bone density parameters measured from a periapical radiograph, CBCT, Micro-CT and histologic analysis

	UA	UP	LA	LP	p-value
Periapical radiograph Total gray value	94.39±22.32	83.39±20.22	117.88±43.90	91.07±32.61	<i>p=0.192</i>
CBCT Total gray density value	1943.68±268.4 5	1784.66±446.87	1769.07±132.01	1848.49±413.55	<i>p=0.648</i>
Micro-CT BV/TV(%)	35.24±10.68	36.11±9.15	63.25±19.86	46.74±13.14	<i>p= 0.000004</i>
Micro-CT Trabecular thickness(mm)	0.1516±0.06	0.1728±0.06	0.2679±0.09	0.2384±0.07	<i>p= 1.8x10⁻⁴</i>
Micro-CT Porosity (%)	64.76±10.68	63.89±0.15	45.84±9.15	53.25±13.14	<i>p= 0.0002</i>
Micro-CT BMD (mg/ccm)	356.72±157.07	341.46±140.50	521.18±210.71	480.76±186.21	<i>p= 0.013</i>
Histologic analysis Bone density (%)	44.55±9.98	40.51±11.54	55.62±9.97	51.61±13.07	<i>p= 0.005</i>

Since the density data from histologic analysis can be considered as a reference value, the bone density showed the difference between the four regions of bone. The LA bone core showed the highest bone density, followed by the LP, UA and UP. All the parameters from periapical radiography, CBCT and Micro-CT revealed the same pattern of bone density. However, the gray value of the periapical radiographs and the gray density value from CBCT could not denote the difference between the 4 bone types.

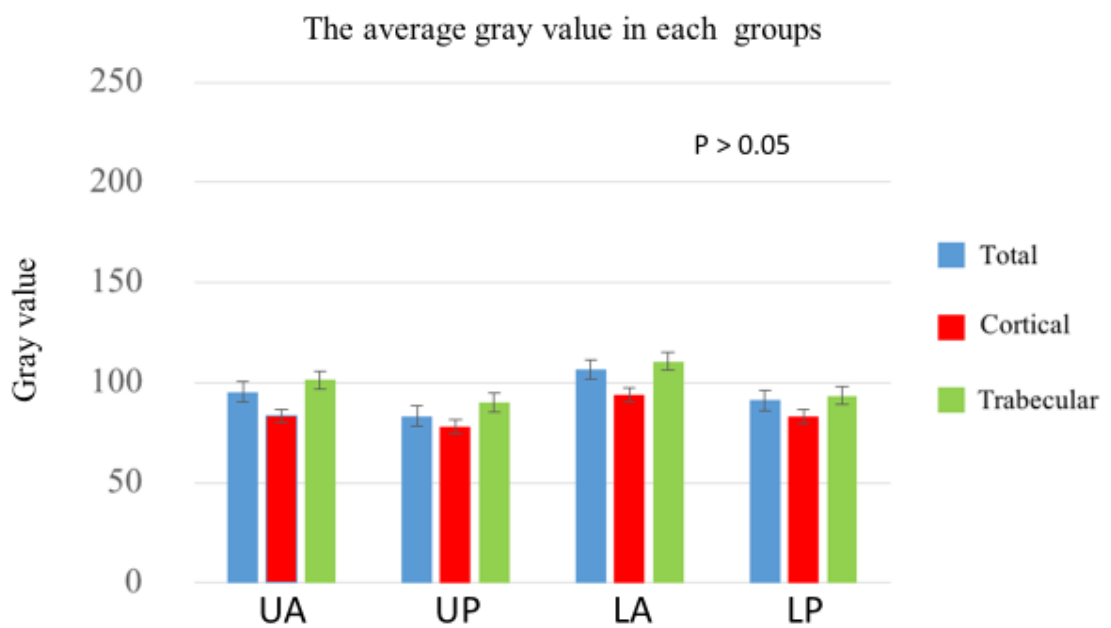


Figure 24: Total, cortical and trabecular gray value from periapical radiograph in each groups

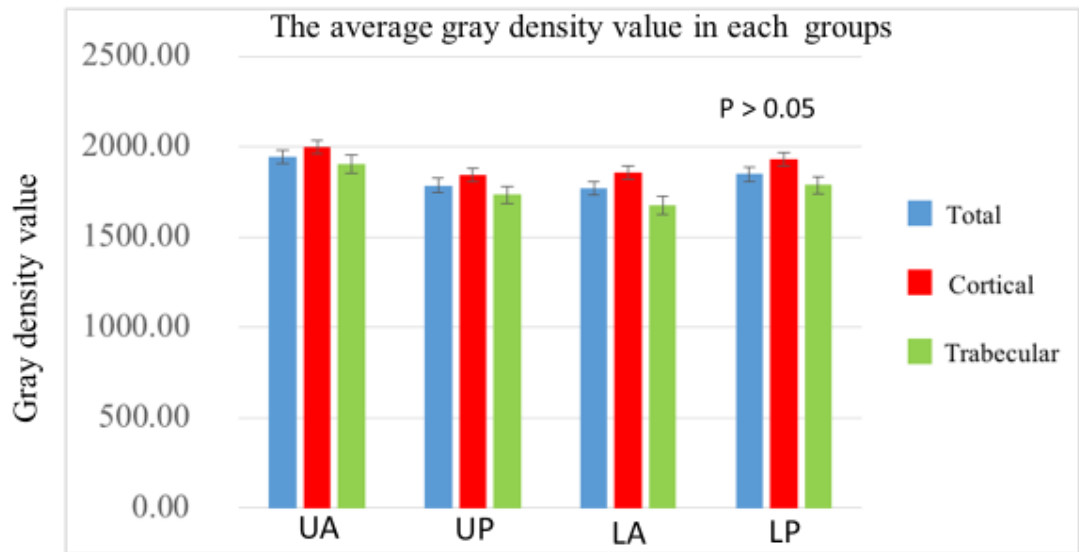


Figure 25: Total, cortical and trabecular gray density value from CBCT in each groups

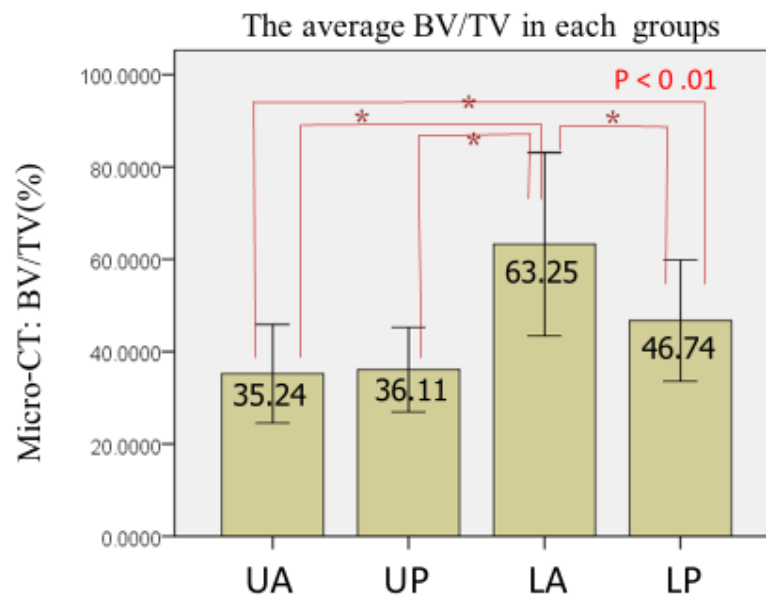


Figure 26: BV/TV (%) from Micro-CT in each groups

The average trabecular thickness in each groups

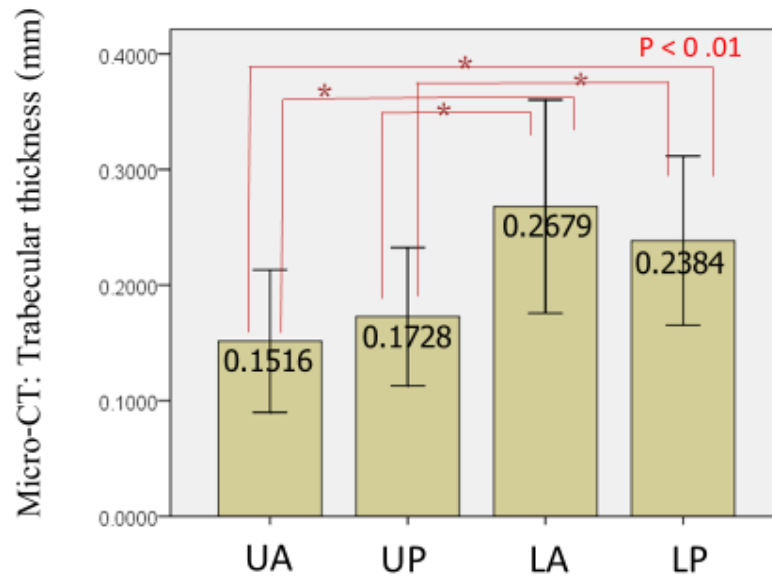


Figure 27: Trabecular thickness (mm) from Micro-CT in each groups

The average porosity in each groups

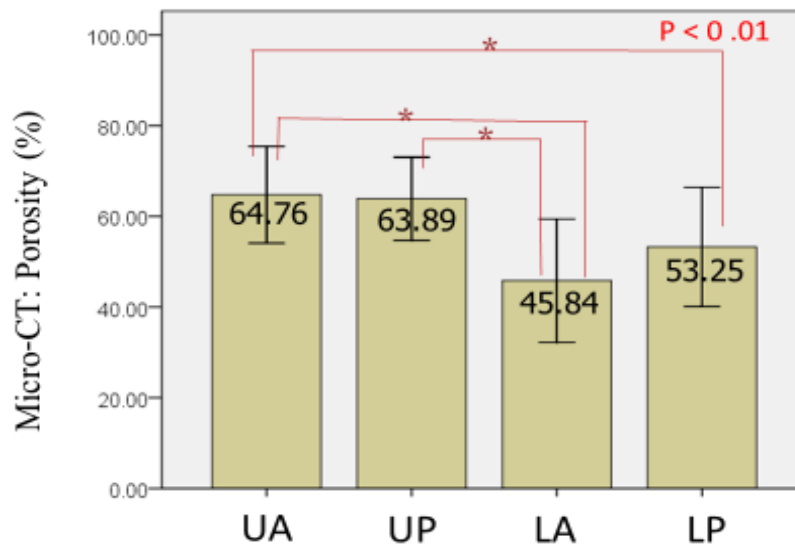


Figure 28: Porosity (%) from Micro-CT in each groups

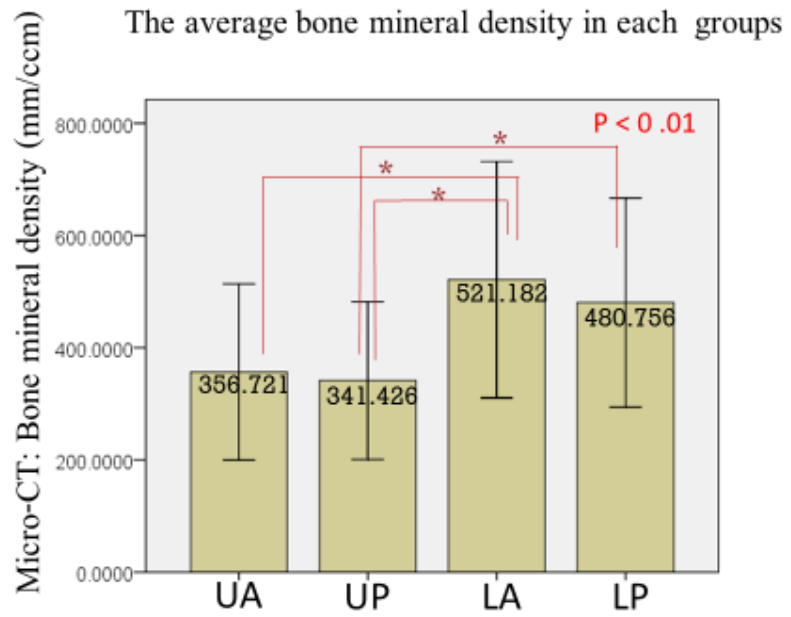


Figure 29: Bone mineral density (mg/ccm) from Micro-CT in each groups

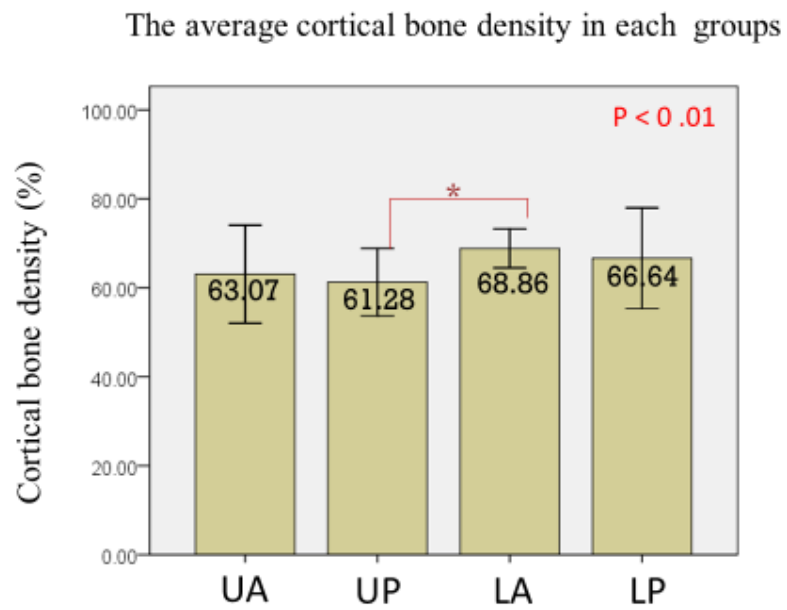


Figure 30: Cortical bone density (%) from histologic analysis in each groups

The average trabecular bone density in each groups

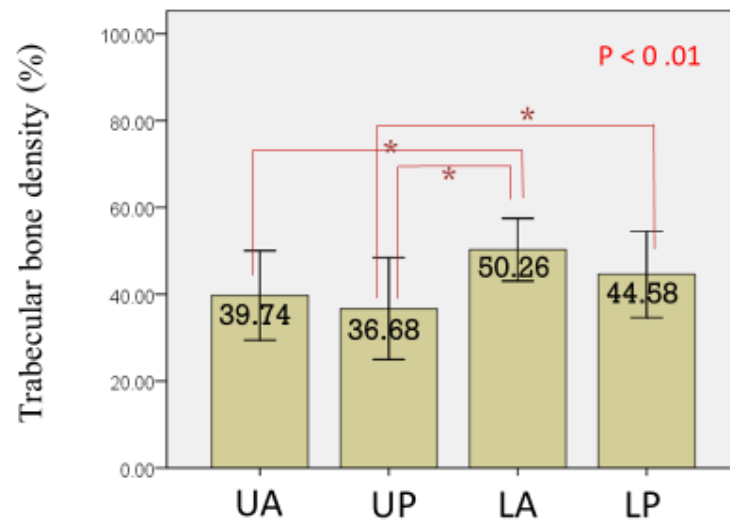


Figure 31: Trabecular bone density (%) from histologic analysis in each groups

The average total bone density in each groups

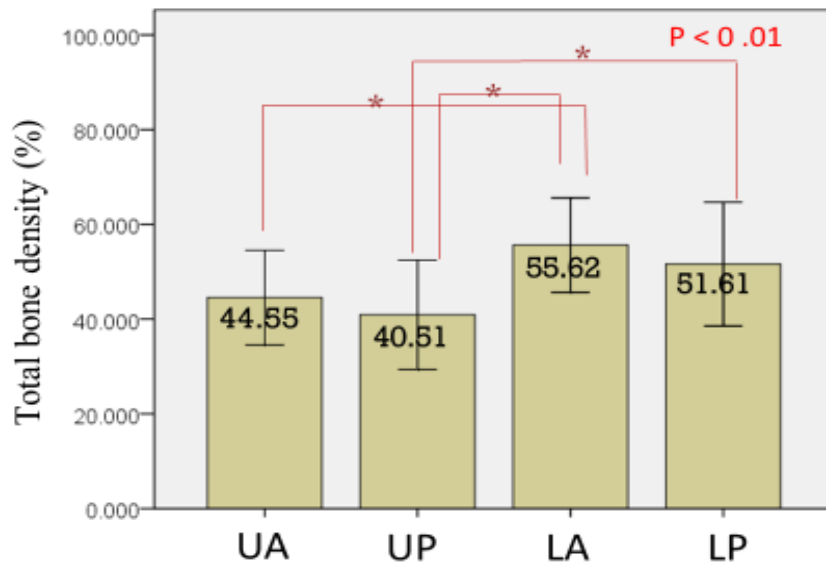


Figure 32: Total bone density (%) from histologic analysis in each groups

The correlation between gray value of periapical radiography and other bone density parameters from CBCT, Micro-CT or histologic analysis

According to the bone density assessment among 4 various technique, there was no correlation between periapical radiography gray value and other bone density parameters from CBCT, Micro-CT or histologic analysis as shown in Table 5 (Figure 33-38).

Table 5: The correlation coefficient between periapical radiography gray value and other bone density parameters from CBCT, Micro-CT or histologic analysis

Periapical	CBCT, Micro-CT and histologic analysis	Coefficient correlation	p-value
Gray value	Gray density value from CBCT	$r = -0.237$	$p = 0.064$
	BV/TV from Micro-CT	$r = 0.107$	$p = 0.408$
	Trabecular thickness Micro-CT	$r = -0.112$	$p = 0.386$
	Porosity from Micro-CT	$r = -0.054$	$p = 0.676$
	BMD from Micro-CT	$r = -0.039$	$p = 0.961$
	Bone density from histologic analysis	$r = -0.006$	$p = 0.765$

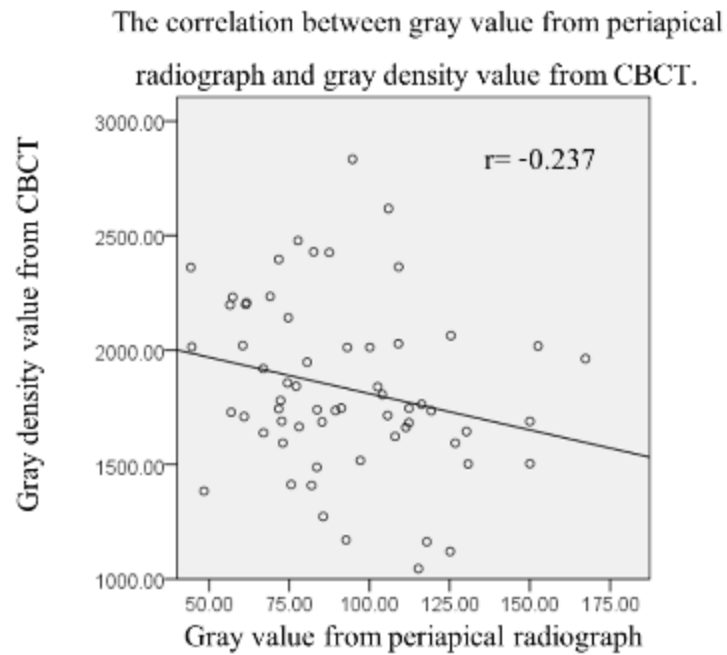


Figure33: The correlation coefficient between gray value from periapical radiograph and gray density value from CBCT

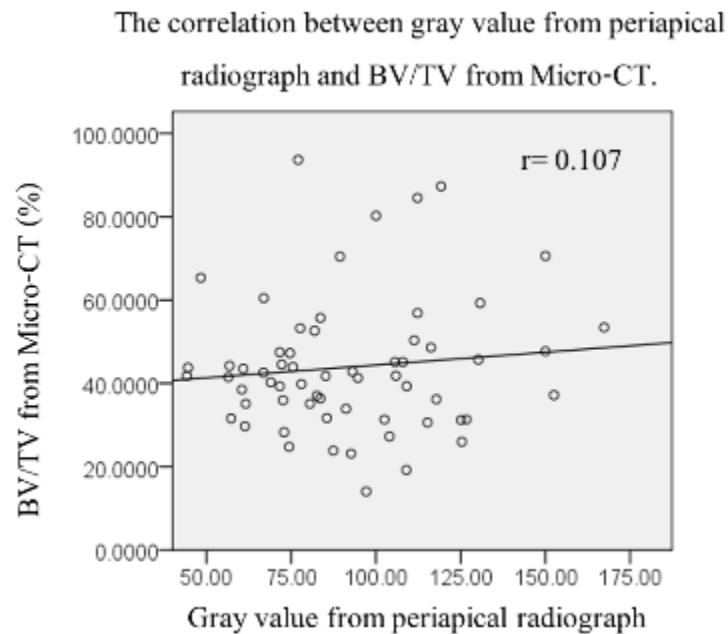


Figure34: The correlation coefficient between gray value from periapical radiograph and BV/TV from Micro-CT

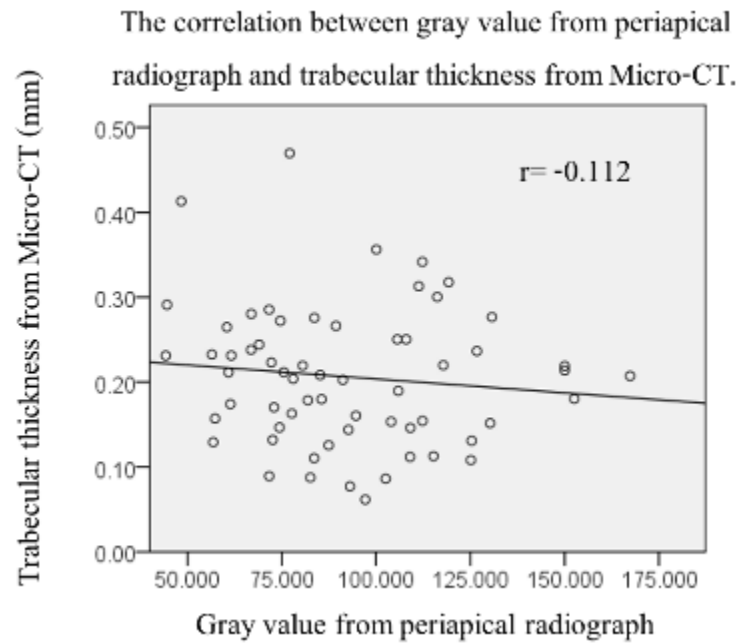


Figure35: The correlation coefficient between gray value from periapical radiograph and trabecular thickness from Micro-CT

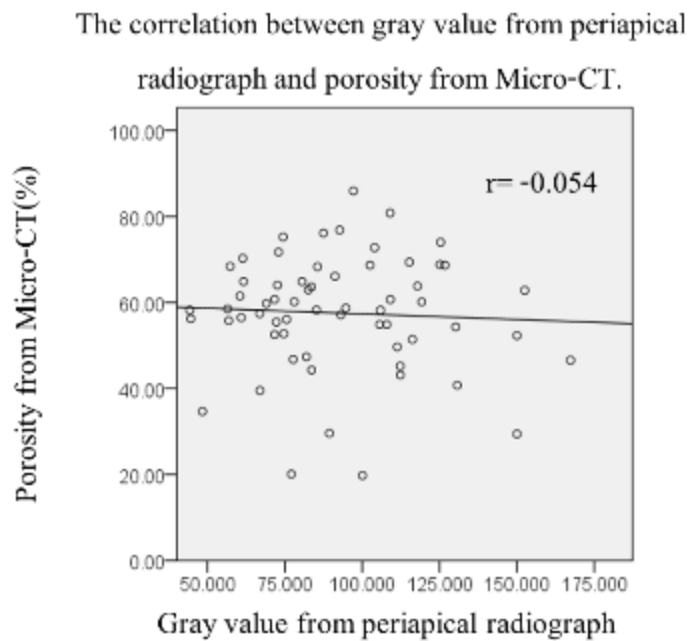


Figure36: The correlation coefficient between gray value from periapical radiograph and porosity from Micro-CT

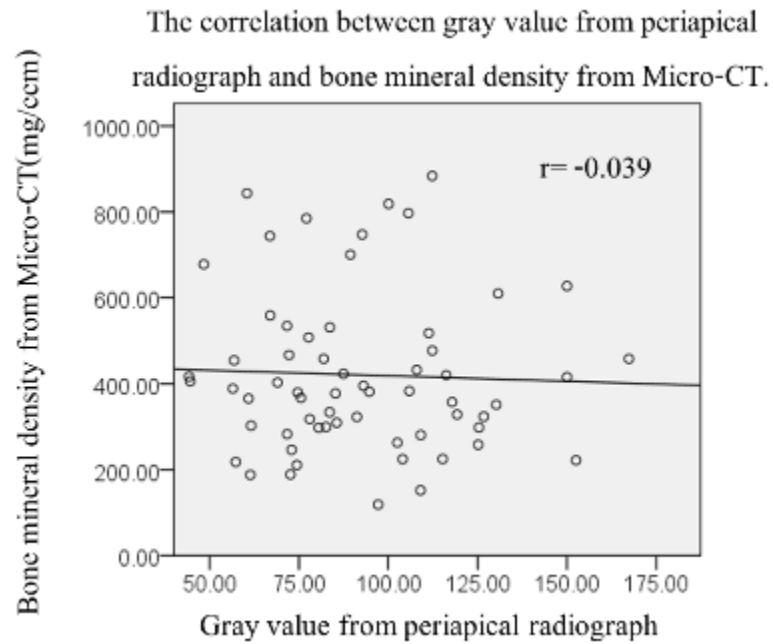


Figure37: The correlation coefficient between gray value from periapical radiograph and bone mineral density from Micro-CT

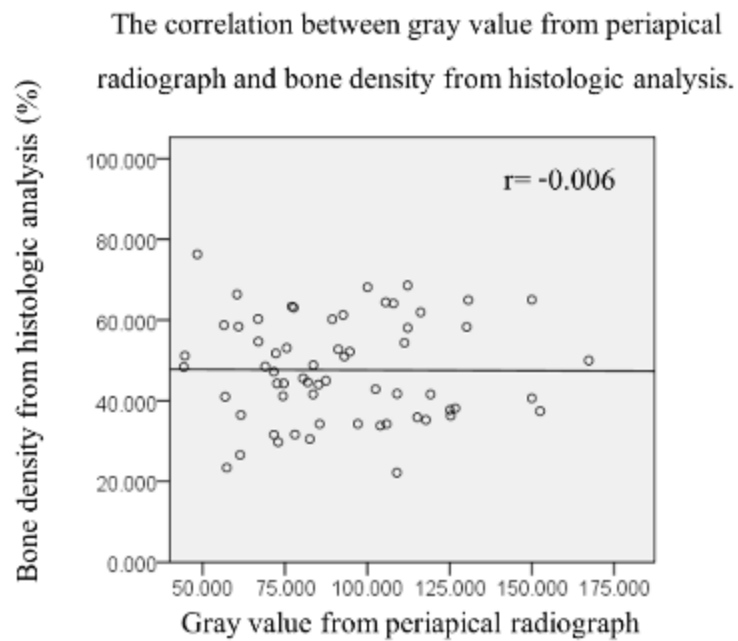


Figure38: The correlation coefficient between periapical radiography gray value and bone density from histologic analysis

The correlation between gray density value of CBCT and other bone density parameters from Micro-CT or histologic analysis

Gray density value measured from CBCT showed no correlation with bone density parameters from Micro-CT or histologic analysis as shown in Table 6 and Figure 39-43.

Table 6: The correlation coefficient of gray density value of CBCT and other bone density parameters from Micro-CT or histologic analysis

CBCT	Micro-CT or histologic analysis	Coefficient correlation	p-value
Gray density value	BV/TV from Micro-CT	$r = -0.057$	$p = 0.657$
	Trabecular thickness Micro-CT	$r = -0.099$	$p = 0.444$
	Porosity from Micro-CT	$r = 0.033$	$p = 0.800$
	BMD from Micro-CT	$r = -0.106$	$p = 0.411$
	Bone density from histologic analysis	$r = -0.135$	$p = 0.294$

The correlation between gray density value from CBCT
and BV/TV from Micro-CT.

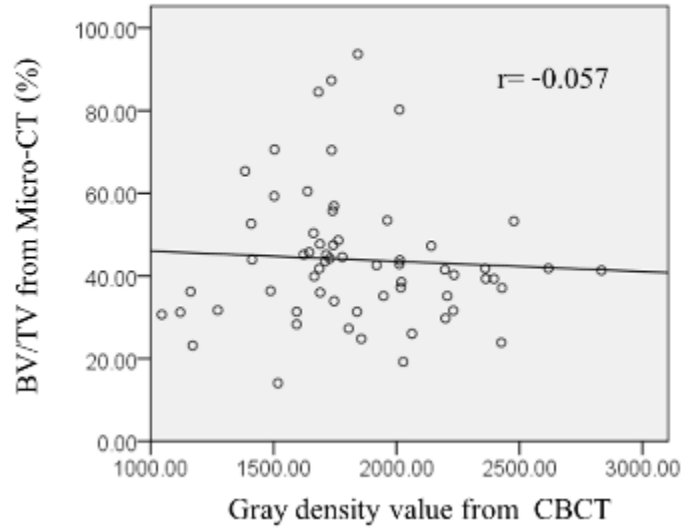


Figure39: The correlation coefficient between gray density value from CBCT and BV/TV from Micro-CT

The correlation between gray density value from CBCT
and trabecular thickness from Micro-CT.

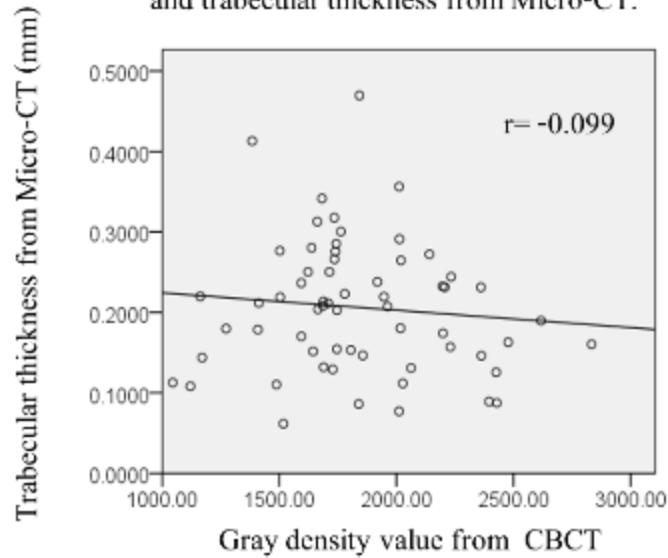


Figure40: The correlation coefficient between gray density value from CBCT and trabecular thickness from Micro-CT

The correlation between gray density value from CBCT
and porosity from Micro-CT.

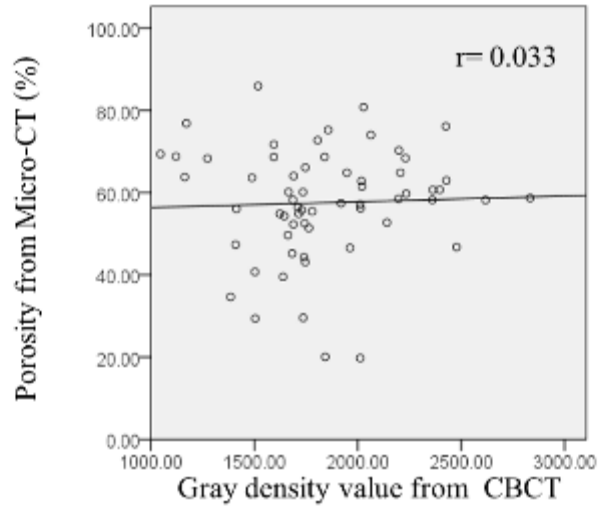


Figure41: The correlation coefficient between gray density value from CBCT and porosity
from Micro-CT

The correlation between gray density value from CBCT
and bone mineral density from Micro-CT.

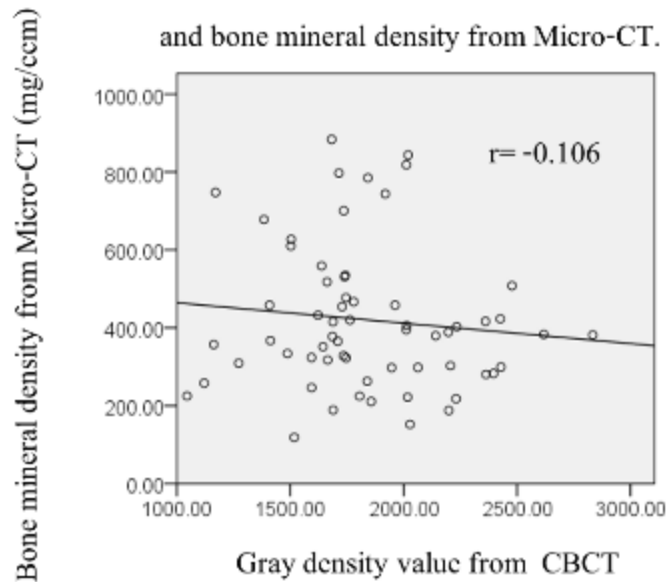


Figure42: The correlation coefficient between gray density value from CBCT and bone mineral
density from Micro-CT

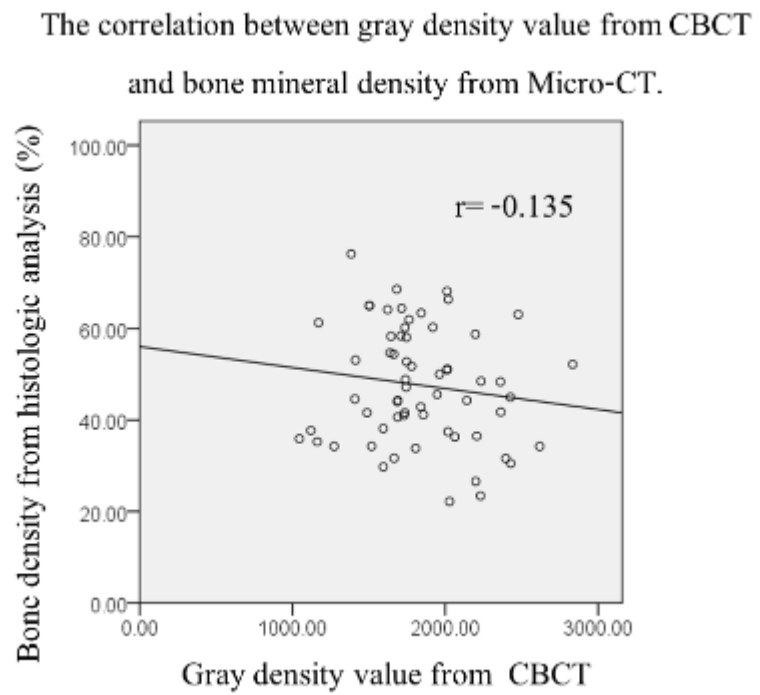


Figure43: The correlation coefficient between gray density value from CBCT and bone density from histologic analysis

The correlation between bone density parameter of Micro-CT and bone density from histologic analysis

There was a positive correlation between bone density parameters from the Micro-CT and bone density parameters from the histologic analysis as shown in Table 7. A high positive Pearson's correlation coefficient was observed between BMD (Micro-CT) and bone density (histologic analysis) ($r=0.812$). The correlation between porosity (Micro-CT) and bone density (histologic analysis) was moderate ($r=-0.683$), as was the correlation between BV/TV (Micro-CT) and bone density (histologic analysis) ($r=0.617$), (Figure 44-46)

Table 7: The correlation coefficient of bone density parameters from Micro-CT and bone density parameters from histologic analysis

Micro-CT	Histologic analysis	Coefficient correlation	p-value
BV/TV	Bone density	$r = 0.617$	$p = 9.47 \times 10^{-8}$
BMD		$r = 0.812$	$p = 1.11 \times 10^{-15}$
Porosity		$r = -0.683$	$p = 9.45 \times 10^{-10}$

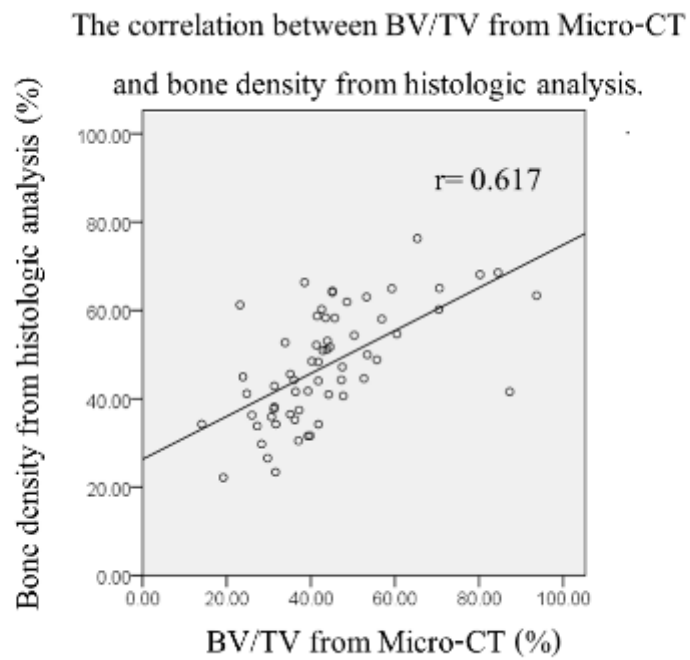


Figure44: The correlation coefficient between BV/TV from Micro-CT and bone density from histologic analysis

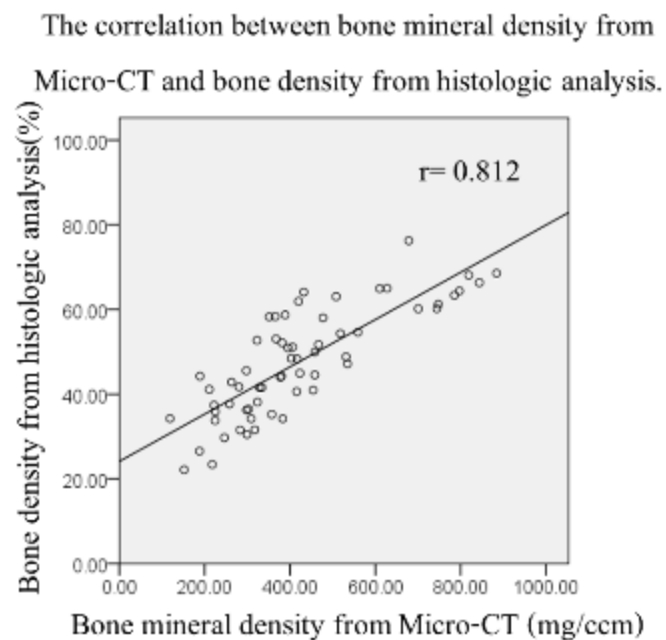


Figure45: The correlation coefficient between bone mineral density from Micro-CT and bone density from histologic analysis

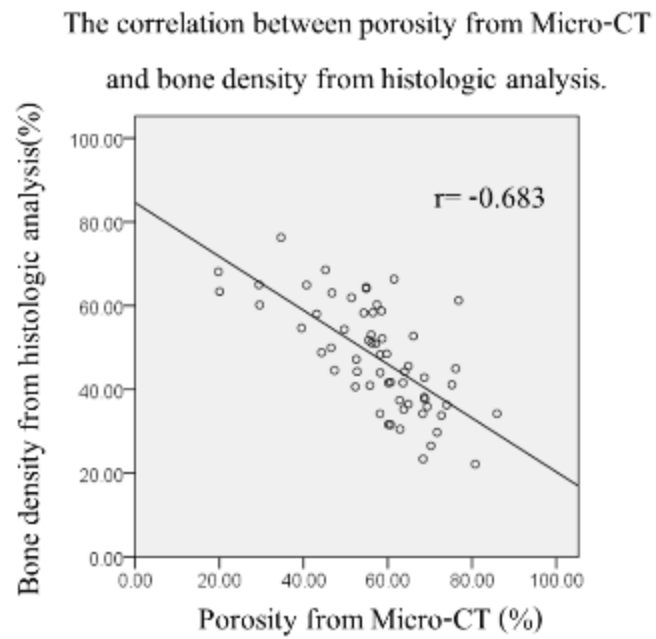


Figure46: The correlation coefficient between porosity from Micro-CT and bone density from histologic analysis

The cortical bone thickness measured from periapical radiography, CBCT and Micro-CT

The cortical bone could not be localized in periapical radiography, so the thickness could not be achieved using this technique.

The cortical bone thickness from CBCT and Micro-CT were demonstrated by means, mean differences, and absolute mean differences between each pair of CBCT and Micro-CT measurement. Pearson's correlation coefficients were calculated for each pair of CBCT and Micro-CT measurement as shown in Table 8. There was no difference for linear measurement between CBCT and Micro-CT evaluation. The UP group showed thinnest cortical bone thickness compared with mandible (LA and LP) ($p < 0.05$) but not difference significant from UA ($p > 0.05$).

Table 8: Measurement accuracy of cortical thickness of 4 regions by means, mean difference (Mean Diff), Absolute value of the mean difference (Mean Abs), standard deviations, and correlations

Location	CBCT Mean±SD (mm)	Micro-CT Mean±SD (mm)	Differences (CBCT-Micro- CT) Mean Diff±SD (mm)	Abs Differences (CBCT-Micro- CT) Mean Abs±SD (mm)	Pearson's Coefficient correlation	p-value
UA	1.01±0.23	1.00±0.25	0.007±0.09	0.078±0.09	0.928	$p = 0.811$
UP	0.87±0.18	0.90±0.18	-0.032±0.10	0.078±0.10	0.842	$p = 0.186$
LA	1.19±0.24	1.20±0.22	-0.08±0.09	0.080±0.09	0.930	$p = 0.783$
LP	1.16±0.25	1.17±0.25	-0.05±0.09	0.095±0.09	0.932	$p = 0.797$
p value	$p = 0.0004$	$p = 0.001$				

Correlation between cortical thickness and bone density

The correlation of CBCT's cortical bone thickness (CBCT) and bone mineral density from Micro-CT was high ($r=0.818$, $r^2=0.669$). There was moderate correlation between cortical thickness (CBCT) and bone density for histologic analysis ($r=0.738$, $r^2=0.545$), BV/TV of Micro-CT ($r=0.634$, $r^2=0.402$), trabecular thickness ($r=0.626$, $r^2=0.392$) and porosity ($r=-0.662$, $r^2=0.438$). The data was demonstrated in Table 9

Table 9: The correlation coefficient of cortical thickness from a CBCT and bone density parameters from Micro-CT and histologic analysis

CBCT	Micro-CT or histologic analysis	Coefficient correlation (r)	(r^2)	p-value
Cortical bone thickness	BV/TV from Micro-CT	$r = 0.634$	0.402	$p = 3 \times 10^{-8}$
	Trabecular thickness	$r = 0.626$	0.392	$p = 8 \times 10^{-13}$
	Porosity from Micro-CT	$r = -0.662$	0.438	$p = 5 \times 10^{-9}$
	BMD from Micro-CT	$r = 0.818$	0.669	$p = 5 \times 10^{-16}$
	Bone density from histologic analysis	$r = 0.738$	0.545	$p = 7 \times 10^{-12}$

The intraoperator reliability for all parameters

The intraclass correlation coefficient ICC value for the 7 continuous variables; gray value (periapical radiograph), gray density value (CBCT), BV/TV (Micro-CT), Trabecular thickness (Micro-CT) %porosity (Micro-CT), bone mineral density (Micro-CT), and bone density (histologic analysis) showed good reliability with coefficients from 0.93 -0.95.

CHAPTER 4

DISCUSSION

The relationship among periapical radiograph- and CBCT- based gray density value, Micro-CT bone density parameters (BMD, BV/TV, %porosity), and bone density from histology analysis were analyzed in this study.

Many studies have confirmed the correlation of Micro-CT and histologic analysis.^{83, 87, 109} Butz and coworkers found that a Micro-CT image corresponded to a histological analysis section from a surface implant to bone contact for cortical bone ($r=0.65$) and trabecular bone ($r=0.92$)¹⁰⁹. Micro-CT and histologic analysis are recommended as the gold standard for imaging bone specimens studies at implant sites⁴⁹. The present study, the bone density parameters from Micro-CT, in particular, BMD showed high coefficient correlation with bone density measured from histology assessment, results that were similarly reported in others studies^{83, 86, 87, 109}. This could confirm a strong correlation and validity between Micro-CT and histologic analysis.

The accuracy of periapical radiography, CBCT, Micro-CT and histologic analysis:

Implications for bone morphology assessment for dental implant placement

For pre-operative dental implant planning, periapical radiographs and CBCTs were the most common radiographs taken to evaluate bone morphology and nearby vital organs. However, these radiographic techniques have limitations; the quality and accuracy of the radiography from each technique vary. There have been variations in periapical radiographs and CBCTs for bone quality measurement in many studies.

The present study also confirmed the limitation of periapical radiograph image for assessment bone quality at the dental implant site. The cortical thickness, that indicates the primary stability of dental implant, could not identify with this radiograph image. Moreover, the periapical radiograph-based gray value was not correlated to bone density parameter from Micro-CT or histology analysis. This is in agreement with the results previously reported by Tanomaru-Filho and coworker in 2009⁹⁶, who concluded that no correlation between periapical radiographic

images compared with histologic images. In addition, periapical radiographs may suffer from distortion, magnification⁵⁸ and image processing⁵³. Errors in demonstrating exact bone density may come from the 2 dimensional-based radiograph, which accumulates the density from the buccal to lingual side. A previous study showed the limitations of periapical radiographs for discriminating various gray density value of hard tissue (enamel, dentine, and bone) resulting in only 44% sensitivity and 78% specificity compared with a Micro-CT for detecting root resorption⁹⁷. A recent study confirmed the inaccuracy of periapical radiographs to validate the size of a bony defect in the jaw bone, showing that the defect size in periapical radiographs was smaller than the histologic image by approximately 10%⁹³. Lia and coworker in 2004 found that the validity of periapical radiographs for measuring periapical lesions ranged from 67.97-76.27%, confirmed by histologic images¹¹². It should be noted that a periapical radiographic image will show only gross details of soft and hard tissue structure without accuracy in size or density of the tissues.

A CBCT is the most commonly used diagnostic tool for evaluating anatomical structure as well as bone architecture prior to dental implant placements. Recently, the American Academy of Oral and Maxillofacial Radiology (AAOMR) updated its guidelines for dental imaging in implant treatment, suggesting a CBCT as the preferred method for pre-surgical assessment of dental implant sites¹¹³. Their recommendations are not mandatory; however, their goal is to give dental professionals a qualified opinion on imaging while reducing radiation risks to the patient.

A CBCT could determine the validity differences between 2D images in insignificant clinical situations¹¹⁴. The measurement error of CBCT was found to range from 1.86-4.61% with no significant difference between the measurements and actual specimens⁶¹. The present study confirmed a high correlation between the CBCT and Micro-CT ($r=0.933$), showing there was 0.94 % difference between a CBCT and Micro-CT for linear measurement. Concerning the mathematical difference of CBCTs and Micro-CTs, the present study found that the specimen showed a difference of about 0.01 mm, which corresponded to Mangione and coworker⁶² that reported a difference of 0.2 mm.

The main drawback of CBCT technology is the lack of appropriate bone determination. Regarding bone density propose, the HU from medical CT scans, which measures radiodensity, can provide an accurate absolute density. Radiodensity is inaccurate in CBCT

scans because different areas in the scan appear with different grayscale value depending on their relative positions to the organ being scanned, despite possessing identical density, because the image value of a voxel of an organ depends on the position in the image volume¹¹⁵. Although some authors have supported the use of a CBCT to evaluate bone density by measuring gray density showing a reliable modality for bone density measurement^{116, 71, 72, 105, 117, 106}, the validity of gray value from a CBCT for bone density measurement is still controversial. The gray density value obtained from CBCT images are not an absolute value like HU value obtained using CT. Katsumata and coworker found that calculated HU on a CBCT scan varied widely from a range of -1500 to over +3000 for different types of bone¹¹⁸. Even after a correction had been applied to gray levels with the CBCT, the HU value were much more reliable than the gray density value obtained from the CBCT^{66, 72, 119}. In addition, Corpas and coworker in 2011 showed that a CBCT was not found to be reliable compared with histologic analysis ($r= 0.28$)⁶⁹. The present study showed a consistent finding that gray value from a CBCT has low validity and no correlation compared with Micro-CT or histologic analysis. It should be taken into consideration that CBCT systems do not employ a standardized system for scaling the gray levels that represent the reconstructed density value and as such, they are arbitrary and do not allow for assessment of bone quality¹²⁰. In the absence of such a standardization, it is difficult to interpret the gray levels or impossible to compare the value resulting from different machines. According to this finding, utilizing data from a CBCT as the tool for evaluation of bone density should be done with caution.

The present study demonstrated a high correlation between cortical bone thickness measured from CBCT and the density of the bone specimen represented either by a Micro-CT (BV/TV; $r=0.634$, porosity; $r=-0.662$, BMD; $r=0.818$) or by bone histologic analysis (bone density from histologic analysis $r=0.818$). Corresponding to Thiele and coworker,¹²¹ a positive correlation between the cortical thickness and bone mineral density (BMD) in cortical and cancellous bone from a Micro-CT measurement in femoral bone was found. The cortical thickness affects the bone density and primary stability. These results suggest that the cortical thickness measured from a CBCT could be used as an indicator for bone density that could represent bone quality at the implant installation site. From this study, it could be assumed that the more cortical bone thickness, the denser the trabecular bone would be.

CHAPTER 5

CONCLUSION

The mandible (LA and LP) revealed the higher cortical thickness and bone density than the maxilla (UA and UP) according to the Micro-CT and histologic analysis. Regarding the bone density evaluation, periapical radiograph- and CBCT-based gray density value could not reveal the true bone density that using BMD, BV/TV, and histology assessment as the references.

The present study demonstrated the strong correlation between the cortical thickness measured from CBCT and the bone density parameters assessed by Micro-CT and histologic analysis. This pre-operative parameter could be utilized as the indicator for bone quality at the implant installation site.

The use of periapical radiograph and CBCT as the preoperative diagnostic tool for dental implant installation should be done with caution. CBCT might be a useful technique for the 2D measurement (the length) rather than the 3D parameter (gray density value).

REFERENCES

1. Esposito M, Hirsch JM, Lekholm U, Thomsen P. Biological factors contributing to failures of osseointegrated oral implants. (II). Etiopathogenesis. *Eur J Oral Sci* 1998; 106(3): 721-64.
2. Esposito M, Hirsch JM, Lekholm U, Thomsen P. Biological factors contributing to failures of osseointegrated oral implants. (I). Success criteria and epidemiology. *Eur J Oral Sci* 1998; 106(1):527-51.
3. Aljehani YA. Diagnostic Applications of Cone-Beam CT for Periodontal Diseases. *Int J Dent* 2014; 2014:865079.
4. Benson BW, Shetty V. Dental Implants, In: Oral Radiology Principles and Interpretation, S.C. White & M. J. Pharoah, pp. 597-612, Mosby, Elsevier, ISBN 978-0-323-04983-2, St. Louis, Missouri. 2009.
5. Chan HL, Misch K, Wang HL. Dental imaging in implant treatment planning. *Implant Dent* 2010; 19(4):288-98.
6. Ekestubbe A, Thilander A, Grondahl HG. Absorbed doses and energy imparted from tomography for dental implant installation. Spiral tomography using the Scanora technique compared with hypocycloidal tomography. *Dentomaxillofac Radiol* 1992; 21(2): 65-9.
7. Ekestubbe A, Thilander A, Grondahl K, Grondahl HG. Absorbed doses from computed tomography for dental implant surgery: comparison with conventional tomography. *Dentomaxillofac Radiol* 1993; 22(1): 13-7.
8. Frederiksen NL, Benson BW, Sokolowski TW. Effective dose and risk assessment from computed tomography of the maxillofacial complex. *Dentomaxillofac Radiol* 1995; 24(1): 55-8.
9. Dula K, Mini R, van der Stelt PF, Lambrecht JT, Schneeberger P, Buser D. Hypothetical mortality risk associated with spiral computed tomography of the maxilla and mandible. *Eur J Oral Sci* 1996; 104(5-6): 503-10.
10. Andersson JE, Svartz K. CT-scanning in the preoperative planning of osseointegrated implants in the maxilla. *Int J Oral Maxillofac Surg* 1988; 17(1): 33-5.

11. Quirynen M, Lamoral Y, Dekeyser C, Peene P, van Steenberghe D, Bonte J, et al. CT scan standard reconstruction technique for reliable jaw bone volume determination. *Int J Oral Maxillofac Implants* 1990; 5(4): 384-9.
12. Feldkamp LA, Goldstein SA, Parfitt AM, Jesion G, Kleerekoper M. The direct examination of three-dimensional bone architecture in vitro by computed tomography. *J Bone Miner Res* 1989; 4(1): 3-11.
13. Naitoh M, Katsumata A, Mitsuya S, Kamemoto H, Ariji E. Measurement of mandibles with microfocus x-ray computerized tomography and compact computerized tomography for dental use. *Int J Oral Maxillofac Implants* 2004; 19(2): 239-46.
14. Liu SM, Zhang ZY, Li JP, Liu DG, Ma XC. [A study of trabecular bone structure in the mandibular condyle of healthy young people by cone beam computed tomography]. *Zhonghua Kou Qiang Yi Xue Za Zhi* 2007;42(6):357-60.
15. Lagravere MO, Carey J, Toogood RW, Major PW. Three-dimensional accuracy of measurements made with software on cone-beam computed tomography images. *Am J Orthod Dentofacial Orthop* 2008; 134(1): 112-6.
16. Hua Y, Nackaerts O, Duyck J, Maes F, Jacobs R. Bone quality assessment based on cone beam computed tomography imaging. *Clin Oral Implants Res* 2009; 20(8): 767-71.
17. Safaee M, Parsa AT, Barbaro NM, Chou D, Mummaneni PV, Weinstein PR, et al. Association of tumor location, extent of resection, and neurofibromatosis status with clinical outcomes for 221 spinal nerve sheath tumors. *Neurosurg Focus* 2015; 39(2): E5.
18. Aksoy U, Eratalay K, Tozum TF. The possible association among bone density values, resonance frequency measurements, tactile sense, and histomorphometric evaluations of dental implant osteotomy sites: a preliminary study. *Implant Dent* 2009; 18(4): 316-25.
19. Stoppie N, Pattijn V, Van Cleynenbreugel T, Wevers M, Vander Sloten J, Ignace N. Structural and radiological parameters for the characterization of jawbone. *Clin Oral Implants Res* 2006; 17(2): 124-33.
20. Nackaerts O, Maes F, Yan H, Couto Souza P, Pauwels R, Jacobs R. Analysis of intensity variability in multislice and cone beam computed tomography. *Clin Oral Implants Res* 2011; 22(8): 873-9.

21. Ribeiro-Rotta RF, Pereira AC, Oliveira GH, Freire MC, Leles CR, Lindh C. An exploratory survey of diagnostic methods for bone quality assessment used by Brazilian dental implant specialists. *J Oral Rehabil* 2010; 37(9): 698-703.
22. Cawood JI, Howell RA. A classification of the edentulous jaws. *Int J Oral Maxillofac Surg* 1988; 17(4): 232-6.
23. Imirzalioglu P, Yuzugullu B, Gulsahi A. Correlation between residual ridge resorption and radiomorphometric indices. *Gerodontology* 2012; 29(2): e536-42.
24. Turkyilmaz I, McGlumphy EA. Influence of bone density on implant stability parameters and implant success: a retrospective clinical study. *BMC Oral Health* 2008; 8: 32.
25. Lekholm U, G.A.Zarb. Patient selection and preparation. Tissue integrated prostheses: osseointegration in clinical dentistry. Edited by: Branemark PI, Zarb GA, Albrektsson T. Chicago: Quintessence Publishing Company; 1985:199-209.
26. Engquist B, Bergendal T, Kallus T, Linden U. A retrospective multicenter evaluation of osseointegrated implants supporting overdentures. *Int J Oral Maxillofac Implants* 1988; 3(2): 129-34.
27. Jaffin RA, Berman CL. The excessive loss of Branemark fixtures in type IV bone: a 5-year analysis. *J Periodontol* 1991; 62(1): 2-4.
28. Misch CE. Density of bone: Effect on treatment planning, surgical approach, and healing. In: Misch, C.E., ed. Contemporary implant dentistry, 469–485. St Louis: Mosby-Year Book, Inc; 1993.
29. Rebaudi A, Trisi P, Cella R, Cecchini G. Preoperative evaluation of bone quality and bone density using a novel CT/microCT-based hard-normal-soft classification system. *Int J Oral Maxillofac Implants* 2010; 25(1): 75-85.
30. Misch CE. Density of bone: A key determinant for treatment planning. In Contemporary Implant Dentistry Edited by: Misch CE. St Louis: Mosby-Year Book; 1999:130-146
31. Misch CE. Divisions of available bone in implant dentistry. *Int J Oral Implantol* 1990; 7(1):9-17.
32. Norton MR, Gamble C. Bone classification: an objective scale of bone density using the computerized tomography scan. *Clin Oral Implants Res* 2001;12(1):79-84.
33. Trisi P, Rao W. Bone classification: clinical-histomorphometric comparison. *Clin Oral Implants Res* 1999; 10(1): 1-7.

34. Cardaropoli G, Lekholm U, Wennstrom JL. Tissue alterations at implant-supported single-tooth replacements: a 1-year prospective clinical study. *Clin Oral Implants Res* 2006; 17(2): 165-71.
35. C.E. M. Density of bone: A key determinant for treatment planning. In Contemporary Implant Dentistry Edited by: Misch CE. St Louis: Mosby-Year Book; 1999:130-146.
36. de Oliveira RC, Leles CR, Normanha LM, Lindh C, Ribeiro-Rotta RF. Assessments of trabecular bone density at implant sites on CT images. *Oral Surg Oral Med Oral Pathol Oral Radiol Endod* 2008; 105(2): 231-8.
37. Roze J, Babu S, Saffarzadeh A, Gayet-Delacroix M, Hoornaert A, Layrolle P. Correlating implant stability to bone structure. *Clin Oral Implants Res* 2009; 20(10): 1140-5.
38. Martinez H, Davarpanah M, Missika P, Celletti R, Lazzara R. Optimal implant stabilization in low density bone. *Clin Oral Implants Res* 2001; 12(5): 423-32.
39. Misch CE, Dietsh-Misch F, Hoar J, Beck G, Hazen R, Misch CM. A bone quality-based implant system: first year of prosthetic loading. *J Oral Implantol* 1999; 25(3): 185-97.
40. Fanghanel J, Proff P, Dietze S, Bayerlein T, Mack F, Gedrange T. The morphological and clinical relevance of mandibular and maxillary bone structures for implantation. *Folia Morphol (Warsz)* 2006; 65(1): 49-53.
41. Turkyilmaz I, Tozum TF, Tumer C. Bone density assessments of oral implant sites using computerized tomography. *J Oral Rehabil* 2007; 34(4): 267-72.
42. Herrmann I, Lekholm U, Holm S, Kultje C. Evaluation of patient and implant characteristics as potential prognostic factors for oral implant failures. *Int J Oral Maxillofac Implants* 2005; 20(2): 220-30.
43. Ulm C, Kneissel M, Schedle A, Solar P, Matejka M, Schneider B, et al. Characteristic features of trabecular bone in edentulous maxillae. *Clin Oral Implants Res* 1999; 10(6): 459-67.
44. Miyamoto I, Tsuboi Y, Wada E, Suwa H, Iizuka T. Influence of cortical bone thickness and implant length on implant stability at the time of surgery--clinical, prospective, biomechanical, and imaging study. *Bone* 2005; 37(6): 776-80.

45. Howashi M, Tsukiyama Y, Ayukawa Y, Isoda-Akizuki K, Kihara M, Imai Y, et al. Relationship between the CT Value and Cortical Bone Thickness at Implant Recipient Sites and Primary Implant Stability with Comparison of Different Implant Types. *Clin Implant Dent Relat Res* 2014.
46. Meira TM, Tanaka OM, Ronsani MM, Maruo IT, Guariza-Filho O, Camargo ES, et al. Insertion torque, pull-out strength and cortical bone thickness in contact with orthodontic mini-implants at different insertion angles. *Eur J Orthod* 2013; 35(6): 766-71.
47. Motoyoshi M, Hirabayashi M, Uemura M, Shimizu N. Recommended placement torque when tightening an orthodontic mini-implant. *Clin Oral Implants Res* 2006; 17(1): 109-14.
48. Wada M, Tsuiki Y, Suganami T, Ikebe K, Sogo M, Okuno I, et al. The relationship between the bone characters obtained by CBCT and primary stability of the implants. *International Journal of Implant Dentistry* 2015; 1(1): 1-7.
49. Ibrahim N, Parsa A, Hassan B, van der Stelt P, Wismeijer D. Diagnostic imaging of trabecular bone microstructure for oral implants: a literature review. *Dentomaxillofac Radiol* 2013; 42(3): 20120075.
50. Southard TE, Wunderle DM, Southard KA, Jakobsen JR. Geometric and densitometric standardization of intraoral radiography through use of a modified XCP system. *Oral Surg Oral Med Oral Pathol Oral Radiol Endod* 1999; 87(2): 253-7.
51. Frederiksen NL. Diagnostic imaging in dental implantology. *Oral Surg Oral Med Oral Pathol Oral Radiol Endod* 1995; 80(5): 540-54.
52. Kavadella A, Karayiannis A, Nicopoulou-Karayianni K. Detectability of experimental peri-implant cancellous bone lesions using conventional and direct digital radiography. *Aust Dent J* 2006; 51(2): 180-6.
53. Nair MK, Ludlow JB, Tyndall DA, Platin E, Denton G. Periodontitis detection efficacy of film and digital images. *Oral Surg Oral Med Oral Pathol Oral Radiol Endod* 1998; 85(5): 608-12.
54. Sewerin IP. Errors in radiographic assessment of marginal bone height around osseointegrated implants. *Scand J Dent Res* 1990; 98(5): 428-33.

55. Misch CE. Density of bone: A key determinant for treatment planning. In Contemporary Implant Dentistry Edited by: Misch CE. St Louis: Mosby-Year Book; 1999:130-146.;1999.
56. Lofthag - Hansen S, Grondahl K, Ekestubbe A. Cone-beam CT for preoperative implant planning in the posterior mandible: visibility of anatomic landmarks. *Clin Implant Dent Relat Res* 2009; 11(3): 246-55.
57. Lofthag-Hansen S. Cone beam computed tomography radiation dose and image quality assessments. *Swed Dent J Suppl* 2010(209): 4-55.
58. Misch CE. Diagnostic imaging and technique. In Contemporary Implant Dentistry Edited by: Misch CE. St Louis: Mosby-Year Book:40-46.;2008.
59. Kircos LT, Misch CE. Diagnostic imaging and techniques. In Contemporary Implant Dentistry Edited by: Misch CE. St Louis, Missouri: Mosby - Year Book; 1999:73-87. ; 1999.
60. De Cock J, Mermuys K, Goubau J, Van Petegem S, Houthoofd B, Casselman JW. Cone-beam computed tomography: a new low dose, high resolution imaging technique of the wrist, presentation of three cases with technique. *Skeletal Radiol* 2012;41(1):93-6.
61. Amin LI, Rahman SA, Alam MK, Daud F. Validity of Cone Beam Computed Tomography (CBCT) on Estimation of Implant Fixture Length. *IMJ* 2013; 20(3): 355-58.
62. Mangione F, Meleo D, Talocco M, Pecci R, Pacifici L, Bedini R. Comparative evaluation of the accuracy of linear measurements between cone beam computed tomography and 3D microtomography. *Ann Ist Super Sanita* 2013; 49(3): 261-5.
63. Baumgaertel S, Palomo JM, Palomo L, Hans MG. Reliability and accuracy of cone-beam computed tomography dental measurements. *Am J Orthod Dentofacial Orthop* 2009; 136(1): 19-25; discussion 25-8.
64. Razi T, Niknami M, Alavi Ghazani F. Relationship between Hounsfield Unit in CT Scan and Gray Scale in CBCT. *J Dent Res Dent Clin Dent Prospects* 2014; 8(2): 107-10.
65. Reeves TE, Mah P, McDavid WD. Deriving Hounsfield units using grey levels in cone beam CT: a clinical application. *Dentomaxillofac Radiol* 2012; 41(6): 500-8.
66. Mah P, Reeves TE, McDavid WD. Deriving Hounsfield units using grey levels in cone beam computed tomography. *Dentomaxillofac Radiol* 2010; 39(6): 323-35.
67. Valiyaparambil JV, Yamany I, Ortiz D, Shafer DM, Pendry D, Freilich M, et al. Bone quality evaluation: comparison of cone beam computed tomography and subjective surgical assessment. *Int J Oral Maxillofac Implants* 2012; 27(5): 1271-7.

68. Lou L, Lagravere MO, Compton S, Major PW, Flores-Mir C. Accuracy of measurements and reliability of landmark identification with computed tomography (CT) techniques in the maxillofacial area: a systematic review. *Oral Surg Oral Med Oral Pathol Oral Radiol Endod* 2007; 104(3): 402-11.
69. Corpas Ldos S, Jacobs R, Quirynen M, Huang Y, Naert I, Duyck J. Peri-implant bone tissue assessment by comparing the outcome of intra-oral radiograph and cone beam computed tomography analyses to the histological standard. *Clin Oral Implants Res* 2011; 22(5): 492-9.
70. Cassetta M, Stefanelli LV, Pacifici A, Pacifici L, Barbato E. How accurate is CBCT in measuring bone density? A comparative CBCT-CT in vitro study. *Clin Implant Dent Relat Res* 2014; 16(4): 471-8.
71. Lagravere MO, Fang Y, Carey J, Toogood RW, Packota GV, Major PW. Density conversion factor determined using a cone-beam computed tomography unit NewTom QR-DVT 9000. *Dentomaxillofac Radiol* 2006; 35(6): 407-9.
72. Naitoh M, Hirukawa A, Katsumata A, Arijii E. Evaluation of voxel values in mandibular cancellous bone: relationship between cone-beam computed tomography and multislice helical computed tomography. *Clin Oral Implants Res* 2009; 20(5): 503-6.
73. Naitoh M, Aimiya H, Hirukawa A, Arijii E. Morphometric analysis of mandibular trabecular bone using cone beam computed tomography: an in vitro study. *Int J Oral Maxillofac Implants* 2010; 25(6): 1093-8.
74. Naitoh M, Hirukawa A, Katsumata A, Arijii E. Prospective study to estimate mandibular cancellous bone density using large-volume cone-beam computed tomography. *Clin Oral Implants Res* 2010; 21(12): 1309-13.
75. Araki K, Okano T. The effect of surrounding conditions on pixel value of cone beam computed tomography. *Clin Oral Implants Res* 2013; 24(8): 862-5.
76. Oliveira ML, Tosoni GM, Lindsey DH, Mendoza K, Tetradis S, Mallya SM. Assessment of CT numbers in limited and medium field-of-view scans taken using Accuitomo 170 and Veraviewepocs 3De cone-beam computed tomography scanners. *Imaging Sci Dent* 2014; 44(4): 279-85.
77. Sennerby L, Wennerberg A, Pasop F. A new microtomographic technique for non-

- invasive evaluation of the bone structure around implants. *Clin Oral Implants Res* 2001; 12(1): 91-4.
78. Engelke K, Graeff W, Meiss L, Hahn M, Delling G. High spatial resolution imaging of bone mineral using computed microtomography. Comparison with microradiography and undecalcified histologic sections. *Invest Radiol* 1993; 28(4): 341-9.
 79. Muller R, Hildebrand T, Ruegsegger P. Non-invasive bone biopsy: a new method to analyse and display the three-dimensional structure of trabecular bone. *Phys Med Biol* 1994; 39(1): 145-64.
 80. Gasser JA, Ingold P, Grosios K, Laib A, Hämmerle S, Koller B. Noninvasive monitoring of changes in structural cancellous bone parameters with a novel prototype micro-CT. *J Bone Miner Metab.* 2005; 23(Suppl): 90-96.
 81. Waarsing JH, Day JH, Weinans H. Longitudinal micro-CT scans to evaluate bone architecture. *J Musculoskelet Neuronal Interact.* 2005; 5(4): 310-12.
 82. Van Oosterwyck H, Duyck J, Vander Sloten J, Van der Perre G, Jansen J, Wevers M, et al. Use of microfocus computerized tomography as a new technique for characterizing bone tissue around oral implants. *J Oral Implantol* 2000; 26(1): 5-12.
 83. Gonzalez-Garcia R, Monje F. Is micro-computed tomography reliable to determine the microstructure of the maxillary alveolar bone? *Clin Oral Implants Res* 2013; 24(7): 730-7.
 84. Chopra PM, Johnson M, Nagy TR, Lemons JE. Micro-computed tomographic analysis of bone healing subsequent to graft placement. *J Biomed Mater Res B Appl Biomater* 2009; 88(2) :611-8.
 85. Hildebrand T, Laib A, Muller R, Dequeker J, Ruegsegger P. Direct three-dimensional morphometric analysis of human cancellous bone: microstructural data from spine, femur, iliac crest, and calcaneus. *J Bone Miner Res* 1999; 14(7): 1167-74.
 86. Bernhardt R, Kuhlisch E, Schulz MC, Eckelt U, Stadlinger B. Comparison of bone-implant contact and bone-implant volume between 2D-histological sections and 3D-SRmicroCT slices. *Eur Cell Mater* 2012; 23: 237-47; discussion 47-8.
 87. Particelli F, Mecozzi L, Beraudi A, Montesi M, Baruffaldi F, Viceconti M. A comparison between micro-CT and histology for the evaluation of cortical bone: effect of

- polymethylmethacrylate embedding on structural parameters. *J Microsc* 2012; 245(3): 302-10.
88. Revell PA. Histomorphometry of bone. *J Clin Pathol* 1983; 36(12): 1323-31.
 89. Muller R, Hahn M, Vogel M, Delling G, Ruegsegger P. Morphometric analysis of noninvasively assessed bone biopsies: comparison of high-resolution computed tomography and histologic sections. *Bone* 1996; 18(3): 215-20.
 90. Wigianto R, Ichikawa T, Kanitani H, Horiuchi M, Matsumoto N, Ishizuka H. Three-dimensional examination of bone structure around hydroxyapatite implants using digital image processing. *J Biomed Mater Res* 1997; 34(2): 177-82.
 91. Akagawa Y, Wadamoto M, Sato Y, Tsuru H. The three-dimensional bone interface of an osseointegrated implant: a method for study. *J Prosthet Dent* 1992; 68(5): 813-6.
 92. Stavropoulos A, Wenzel A. Accuracy of cone beam dental CT, intraoral digital and conventional film radiography for the detection of periapical lesions. An ex vivo study in pig jaws. *Clin Oral Investig* 2007; 11(1): 101-6.
 93. Christiansen R, Kirkevang LL, Gotfredsen E, Wenzel A. Periapical radiography and cone beam computed tomography for assessment of the periapical bone defect 1 week and 12 months after root-end resection. *Dentomaxillofac Radiol* 2009; 38(8): 531-6.
 94. Hassan BA. Reliability of periapical radiographs and orthopantomograms in detection of tooth root protrusion in the maxillary sinus: correlation results with cone beam computed tomography. *J Oral Maxillofac Res* 2010; 1(1): e6.
 95. Liang YH, Jiang L, Gao XJ, Shemesh H, Wesselink PR, Wu MK. Detection and measurement of artificial periapical lesions by cone-beam computed tomography. *Int Endod J* 2014; 47(4): 332-8.
 96. Tanomaru-Filho M, Jorge EG, Duarte MA, Goncalves M, Guerreiro-Tanomaru JM. Comparative radiographic and histological analyses of periapical lesion development. *Oral Surg Oral Med Oral Pathol Oral Radiol Endod* 2009; 107(3): 442-7.
 97. Dudic A, Giannopoulou C, Martinez M, Montet X, Kiliaridis S. Diagnostic accuracy of digitized periapical radiographs validated against micro-computed tomography scanning in evaluating orthodontically induced apical root resorption. *Eur J Oral Sci* 2008; 116(5): 467-72.
 98. Amouriq Y, Evenou P, Arlicot A, Normand N, Layrolle P, Weiss P, et al. Evaluation of

- trabecular bone patterns on dental radiographic images:influence of cortical bone. SPIE Medical Imaging, Feb 2010, United States. 10 p.,2010.
99. Arisan V, Karabuda ZC, Avsever H, Ozdemir T. Conventional multi-slice computed tomography (CT) and cone-beam CT (CBCT) for computer-assisted implant placement. Part I: relationship of radiographic gray density and implant stability. *Clin Implant Dent Relat Res* 2013; 15(6): 893-906.
 100. Soardi CM, Bianchi AE, Zandanel E, Spinato S. Clinical and radiographic evaluation of immediately loaded one-piece implants placed into fresh extraction sockets. *Quintessence Int* 2012; 43(6): 449-56.
 101. Ho JT, Wu J, Huang HL, Chen MY, Fuh LJ, Hsu JT. Trabecular bone structural parameters evaluated using dental cone-beam computed tomography: cellular synthetic bones. *Biomed Eng Online* 2013; 12: 115.
 102. Parsa A, Ibrahim N, Hassan B, Motroni A, van der Stelt P, Wismeijer D. Influence of cone beam CT scanning parameters on grey value measurements at an implant site. *Dentomaxillofac Radiol* 2013; 42(3): 79884780.
 103. Livada R. Histomorphometric and bone densitometric analysis of dental implant site Faculty of The University of Alabama at Birmingham; 2009.
 104. Leavitt C. Correlation of bone density using histomorphometric and cone beam computed tomographic analysis Birmingham University of Alabama at Birmingham; 2010.
 105. Huang Y, Dessel JV, Depypere M, EzEldeen M, Iliescu AA, Santos ED, et al. Validating cone-beam computed tomography for peri-implant bone morphometric analysis. *Bone Res* 2014; 2: 14010.
 106. Lee CY, Prasad HS, Suzuki JB, Stover JD, Rohrer MD. The correlation of bone mineral density and histologic data in the early grafted maxillary sinus: a preliminary report. *Implant Dent* 2011; 20(3): 202-14.
 107. Monje A, Monje F, Gonzalez-Garcia R, Galindo-Moreno P, Rodriguez-Salvanes F, Wang HL. Comparison between microcomputed tomography and cone-beam computed tomography radiologic bone to assess atrophic posterior maxilla density and microarchitecture. *Clin Oral Implants Res* 2014; 25(6): 723-8.
 108. Hsu JT, Chen YJ, Ho JT, Huang HL, Wang SP, Cheng FC, et al. A comparison of micro-CT and dental CT in assessing cortical bone morphology and trabecular bone

- microarchitecture. *PLoS One* 2014; 9(9): e107545.
109. Butz F, Ogawa T, Chang TL, Nishimura I. Three-dimensional bone-implant integration profiling using micro-computed tomography. *Int J Oral Maxillofac Implants* 2006; 21(5): 687-95.
 110. Becker K, Stauber M, Schwarz F, Beissbarth T. Automated 3D-2D registration of X-ray microcomputed tomography with histological sections for dental implants in bone using chamfer matching and simulated annealing. *Comput Med Imaging Graph* 2015; 44:62-8.
 111. Erpenstein H, Diedrich P, Borchard R. Preparation of autogenous bone grafts in two different bone mills. *Int J Periodontics Restorative Dent* 2001; 21(6): 609 - 15.
 112. Lia RC, Garcia JM, Sousa-Neto MD, Saquy PC, Marins RH, Zuccolotto WG. Clinical, radiographic and histological evaluation of chronic periapical inflammatory lesions. *J Appl Oral Sci* 2004; 12(2): 117-20.
 113. Tyndall DA, Brooks SL. Selection criteria for dental implant site imaging: a position paper of the American Academy of Oral and Maxillofacial radiology. *Oral Surg Oral Med Oral Pathol Oral Radiol Endod* 2000; 89(5): 630-7.
 114. Al-Ekrish AA, Ekram M. A comparative study of the accuracy and reliability of multidetector computed tomography and cone beam computed tomography in the assessment of dental implant site dimensions. *Dentomaxillofac Radiol* 2011; 40(2): 67-75.
 115. Swennen GR, Schutyser F. Three-dimensional cephalometry: spiral multi-slice vs cone-beam computed tomography. *Am J Orthod Dentofacial Orthop* 2006; 130(3): 410-6.
 116. Aranyarachkul P, Caruso J, Gantes B, Schulz E, Riggs M, Dus I, et al. Bone density assessments of dental implant sites: 2. Quantitative cone-beam computerized tomography. *Int J Oral Maxillofac Implants* 2005; 20(3): 416-24.
 117. Soardi CM, Zaffe D, Motroni A, Wang HL. Quantitative comparison of cone beam computed tomography and microradiography in the evaluation of bone density after maxillary sinus augmentation: a preliminary study. *Clin Implant Dent Relat Res* 2014; 16(4): 557-64.
 118. Katsumata A, Hirukawa A, Okumura S, Naitoh M, Fujishita M, Arijji E, et al. Effects of image artifacts on gray-value density in limited-volume cone-beam computerized tomography. *Oral Surg Oral Med Oral Pathol Oral Radiol Endod* 2007; 104(6): 829-36.

119. Nomura Y, Watanabe H, Honda E, Kurabayashi T. Reliability of voxel values from cone-beam computed tomography for dental use in evaluating bone mineral density. *Clin Oral Implants Res* 2010; 21(5): 558-62.
120. Lee S, Gantes B, Riggs M, Crigger M. Bone density assessments of dental implant sites: 3. Bone quality evaluation during osteotomy and implant placement. *Int J Oral Maxillofac Implants* 2007; 22(2): 208-12.
121. Thiele OC, Eckhardt C, Linke B, Schneider E, Lill CA. Factors affecting the stability of screws in human cortical osteoporotic bone: a cadaver study. *J Bone Joint Surg Br* 2007; 89(5): 701-5.

APPENDIX

ที่ ศธ 0521.1.03/ 0337



คณะทันตแพทยศาสตร์
มหาวิทยาลัยสงขลานครินทร์
ตู้ไปรษณีย์เลขที่ 17
ที่ทำการไปรษณีย์โทรเลขคอหงส์
อ.หาดใหญ่ จ.สงขลา 90112

หนังสือฉบับนี้ให้ไว้เพื่อรับรองว่า

โครงการวิจัยเรื่อง "การเปรียบเทียบภาพถ่ายรังสีปลายรากฟัน โคนบีมซีที ไมโครซีที และโครงสร้างเนื้อเยื่อในการประเมินคุณภาพของกระดูกในตำแหน่งที่ใส่รากฟันเทียม"

รหัสโครงการ EC5701-06-P- HR

หัวหน้าโครงการ ทันตแพทย์ประติพัทธ์ เลือเป็ย

สังกัดหน่วยงาน นักศึกษาหลังปริญญา ภาควิชาศัลยศาสตร์ คณะทันตแพทยศาสตร์ มหาวิทยาลัยสงขลานครินทร์

ได้ผ่านการพิจารณาและได้รับความเห็นชอบจากคณะกรรมการจริยธรรมในการวิจัย (Research Ethics Committee) ซึ่งเป็นคณะกรรมการพิจารณาการศึกษาการวิจัยในคนของคณะทันตแพทยศาสตร์ มหาวิทยาลัยสงขลานครินทร์ ดำเนินการให้การรับรองโครงการวิจัยตามแนวทางหลักจริยธรรมการวิจัยในคนที่เป็นสากล ได้แก่ Declaration of Helsinki, the Belmont Report, CIOMS Guidelines และ the International Conference on Harmonization in Good Clinical Practice (ICH-GCP)

ในคราวประชุมครั้งที่ 1/2557 เมื่อวันที่ 20 กุมภาพันธ์ 2557

ให้ไว้ ณ วันที่ 24 ส.ค. 2557

(ผู้ช่วยศาสตราจารย์ ดร.ทพญ.ศรีสุรางค์ สุทธิปรียาศรี)

ประธานคณะกรรมการจริยธรรมในการวิจัย

.....กรรมการ
(ผู้ช่วยศาสตราจารย์ ทพ.นพ.สุรพงษ์ วงศ์วิชานนท์)

.....กรรมการ
(อาจารย์ ดร. ทพญ.สุพัชรินทร์ พิวัฒน์)

.....กรรมการ
(รองศาสตราจารย์ นพ.พรชัย สติระปัญญา)

.....กรรมการ
(อาจารย์ ทพ.กมลพันธ์ เนื่องศรี)

.....กรรมการ
(ผู้ช่วยศาสตราจารย์ ดร.ทพญ.อังคณา เขียวมนตรี)

.....กรรมการ
(อาจารย์วศิน สุวรรณรัตน์)

.....กรรมการ
(ผู้ช่วยศาสตราจารย์ ดร.ทพญ.สุวรรณ จิตภักดิ์ดินทร์)

VITAE

Name Pradipat Suapear

Student ID 5610820006

Education Attainment

Degree	Name of institute	Year of Graduate
Doctor of Dental Surgery	Prince of Songkla University	2008
Higher Graduate Diploma in Clinical Science (Oral and Maxillofacial Surgery)	Prince of Songkla University	2012

Work-Position and Address

Dentist of Special Expertise in Department of Dentistry, Phunphin Hospital,
Amphoe Phunphin

List of Publication and Proceeding

Suapear P., Leepong N., Suttapreyasri S. Bone quality evaluation at dental
implant site using cone beam computed tomography: correlation results with micro computed
tomography. **The 8th Silpakorn University International Conference on Academic Research
and Creative Arts: Integration of Art and Science.**